CHAPTER 2: LITERATURE REVIEW

2.1 General

This chapter is divided in to two parts. The first part contains a brief overview of the mechanism of bond, anchorage of bars, and the behavior of joint lap splices. Also, it includes the main equations and recommendations given by different international building codes for lap splices. These codes are ECP 203-2007[9], ACI 318-2014[2], Eurocode 2-2004[10], and Canadian Standards CSA A23.3-04[7]. Also, this part contains a review of some of the previous experimental studies dealing with tension lap splices of conventional anchorage of reinforcing bars. The second part contains a description of the headed bars, the mechanism of headed bars, development length of headed bars and the behavior of lap splices. Also, it includes the main equations and recommendations given by the American code ACI 318-14[2] and Canadian Standards CSA A23.3-04[7]. Moreover, this part contains a review of some types of headed bar and the previous experimental studies dealing with the behavior of headed reinforcement bars and its application in reinforced concrete structures.

2.2 Bond and anchorage of bars without head

2.2.1 Basic Consideration

Since external load is very rarely applied directly to the reinforcement, steel can receive its share of the load only from the surrounding concrete. "Bond stress" is the name assigned to the shear stress at the bar-concrete interface which, by transferring load between the bar and the surrounding concrete, affects the steel stresses. This bond, when efficiently developed, enables the two materials to form a composite element. The attainment of satisfactory performance in bond is the most important aim of the detailing of reinforcement in structural concrete elements.

Bond forces are measured by the rate of change in the force in reinforcing bars. Bond stress will not exist unless the steel stresses change between any two sections. Bond stress **u**, customarily defined as a shear force per unit area of bar surface, is given by

$$u = \frac{q}{\sum o} = \frac{\Delta f_s A_b}{\sum o} = \frac{d_b}{4}\,\Delta f_s \quad \text{..... (2.1)}$$

where:

q= change of bar force over unit length.

$\sum 0$ = nominal surface area of a bar of unit length.

d_b= nominal diameter of the bar.

Δf_s= change of steel stress over unit length.

A_b =area of bar.

2.2.2 The mechanism of bond in tension bars

Bond refers to the interaction between reinforcing steel and the surrounding concrete that allows for transfer of tensile stress from the steel into the concrete. Bond influences many other important features of structural concrete such as crack control and section stiffness.

Figure (2-1) shows a straight bar embedded into a block of concrete. When the bond stress is sufficient to resist design tensile loads in the bar, then the force in the bar is "developed" and the embedment length necessary for anchorage of the fully stressed reinforcing bar is referred to as its development length.

Deformed reinforcing bars develop bond stresses by means of transverse ribs that bear directly on the concrete. As tensile forces develop in a reinforcing bar, transverse cracks propagate from the edges of the ribs. This was experimentally shown by Goto (1971) [12], and is reproduced in Fig. (2-2).The bond stress produced by the bearing of the ribs is not uniform. Figure (2-2) also shows the distribution of tensile and bond stresses for the bar. It is important to note that a bar does not uniformly yield in cracked concrete when it is properly bonded. Yielding occurs only locally near cracks. The transverse cracking shown in Fig. (2-2) causes the bearing stresses on the ribs to act along a direction parallel to the transverse crack angle and not parallel with the axis of the bar. Figure (2-3-i) shows bearing stresses acting at an angle, θ_{bond}, relative to the bar axis. These bearing forces can be analyzed into parallel and perpendicular components, as shown in Fig. (2-3-ii). The components parallel to the bar constitute the bond responsible for resisting the tensile force in the reinforcement. The components perpendicular to the bar act outward from the bar surface as splitting stresses on the concrete. These radial splitting stresses must be counteracted by ring tension stresses in the concrete surrounding the reinforcing bar, section A-A of Fig. (2-3-iii). Ultimately, the radial splitting stresses exceed the tensile capacity of the surrounding concrete and splitting cracks begin to propagate from the bar surface.

Bond can fail in multiple ways. The longitudinal bond stresses can exceed the shear strength of the concrete keys between ribs and the bar can pull free. This is referred to as a "pullout" failure (It is also sometimes termed a "shear-out" failure). More commonly though, splitting cracks will propagate from the bar to the surface of the concrete and the cover will spill off. Figure (2-4) and Fig. (2-5) show some of the many splitting cracks that can occur. The type of splitting failure that occurs in unconfined concrete is governed by bar spacing and cover dimensions. Beyond a certain level of splitting resistance, pullout failure will govern. Typically though, splitting resistance governs the level of bond stress that concrete can sustain. As a rib begins to bear on the concrete, a wedge of crushed paste is formed in front of the rib. This wedge acts to change the effective face angle of the rib as shown in Fig. (2-6). The effect of this is that radial splitting stresses tend to increase at a rate greater than the longitudinal bond stresses as tensile load in the reinforcing bar rises.

Rib bearing area can be increased by manipulating one or both of two geometric parameters: the height of the ribs or the spacing of the ribs. Rib bearing area is generally referred to by the ratio of rib bearing area to shearing area of the concrete keys between successive ribs. This ratio is referred to as the relative rib area, R_r (ratio of projected rib area normal to bar axis to the product of the nominal bar perimeter and the center-to-center rib spacing).

2.2.3 Development length equations in some international building Codes

2.2.3.1 Egyptian code 203-2007[9]

The development length for tension (L_d) is calculated using the following equation:

$$L_d = \left(\frac{\alpha.\beta.\eta.f_y/1.15}{4.f_{bu}} \right) d_b \quad \text{..... (2.2)}$$

Where:

f_{bu}: The bond stress $= 0.3 \sqrt{\frac{f_{cu}}{1.5}}$

d_b = bar diameter.

$\eta = 1.30$ For horizontal tensioned bars where thickness of underneath concrete is greater than 300 mm, and is equal to 1.0 for other cases.

α = bar end condition (straight or with hook).

β = surface of the bar condition coefficient (plain or deformed).

In all cases, the development length; L_d, should not be less than 35 d_b or 400 mm whichever is greater for plain bars with hooks, and should not be less than 40 d_b or 300 mm whichever is greater for deformed bars.

2.2.3.2 ACI 318-14[2]

The development length for tension (L_d) is calculated using the following equation:

$$L_d = \left(\frac{f_y}{1.1\lambda\sqrt{fc'}} * \frac{\Psi_t \Psi_e \Psi_s}{\left(\frac{C_b + K_{tr}}{d_b}\right)} \right) d_b \quad \text{..... (2-3)}$$

With $\frac{C_b + k_{tr}}{d_b} \leq 2.5$, and

$$k_{tr} = \frac{40A_{tr}}{sn} \quad \text{..... (2-4)}$$

Where:

L_d = development length of bar (mm).

d_b = nominal bar diameter (mm).

f_y = yield stress of reinforcing steel being developed (MPa).

f_c' = cylinder compressive stress of concrete (MPa).

Ψ_t = reinforcement location factor (1.3 if 300 mm of concrete cast below bar).

Ψ_e = coating factor (1.5 for epoxy -coated bars with minimum clear dimension $\leq 3\ d_b$, or clear spacing less than 6 d_b, 1.2 for all other epoxy-coated bars and 1.0 for uncoated and galvanized reinforcement).

Ψ_s= reinforcement size factor (0.8 for d_b = 19 mm deformed bars and smaller).

λ = lightweight aggregate concrete factor ($\leq$ 0.75 for lightweight aggregates).

c_b = minimum spacing or cover dimension.

k_{tr} = transverse reinforcement index.

s = maximum spacing of transverse reinforcement within L_d, center-to-center.

n = number of bars or wires being developed along the plane of splitting.

A_{tr} = total area of transverse reinforcement within the spacing, s, that crosses the plane of splitting through the reinforcement being developed (mm^2).

It shall be permitted to use k_{tr} = 0.0 as a design simplification even if transverse reinforcement is present.

2.2.3.3 Eurocode 2-2004[10]

The development length for tension (L_d) is calculated using the following equation:

$$L_d = \frac{d_b}{4} * \frac{f_s}{f_{bd}} \quad \text{..... (2-5)}$$

Where:

L_d = development length of bar (mm).

d_b = nominal bar diameter (mm).

f_s = the design stress in the bar.

f_{bd} = the design value of the ultimate bond stress = 2.25 η_1 η_2 f_{ctd} .

Where:

f_{ctd} = the design value of concrete tensile strength.

η_1 = a coefficient related to the quality of the bond condition and the position of bar:

η_1 = 1.0 when "good" conditions are obtained and η_1 = 0.7 for all other cases.

η_2 = a coefficient related to the bar diameter:

η_2 = 1.0 for $d_b \leq$ 32 mm and η_2 = (132-d_b) / 100 for $d_b >$ 32 mm.

2.2.3.4 Canadian code A23.3-04[7]

The development length of deformed bars in tension shall be determined from Equation (2-6) or the simplified Equation (2-7) but (L_d) shall be not less than 300 mm:

$$L_d = 1.15 \frac{k_1 k_2 k_3 k_4}{(d_{cs} + k_{tr})} \frac{f_y}{\sqrt{f_c'}} A_b \quad \text{..... (2-6)}$$

The development length (L_d) of deformed bars in tension may be taken from Equation (2-7) provided that the clear cover and clear spacing of the bars being developed are at least d_b and 1.4 d_b, respectively.
For member containing minimum ties or minimum stirrups within slabs, walls, shells, or folded plates having clear spacing of not less than 2 d_b between bars being developed.

$$L_d = 0.45\, k_1\, k_2\, k_3\, k_4 \frac{f_y}{\sqrt{f_c'}} d_b \quad \text{...} \quad (2\text{-}7)$$

Where:

k_1 is the bar location factor:
= 1.3 for horizontal reinforcement placed in such a way that more than 300 mm of fresh concrete is cast in the member below the development length or splice.
= 1.0 for other cases.

k_2 is a coating factor:
=1.5 for epoxy-coated reinforcement with clear covers less than 3 d_b, or with clear spacing between bars being developed less than 6 d_b.
= 1.2 for all other epoxy-coated reinforcement.
= 1.0 for uncoated reinforcement.

k_3 is the concrete density factor:
= 1.3 for structural low-density concrete.
= 1.2 for structural semi-low-density concrete.
= 1.0 for normal-density concrete.

k_4 is the bar size factor:
= 0.8 for 20 mm and smaller bars and deformed wires.
= 1.0 for 25 mm and larger bars.

$k_{tr} = \frac{A_{tr}\, f_{yt}}{10.5\, sn}$, and ($d_{cs}$+ k_{tr})$\leq 2.5 d_b$, the product (k_1 k_2) need not be taken greater than (1.7).

k_{tr} = transverse reinforcement index.

f_{yt} = yield stress of transverse reinforcement being developed (MPa).

A_{tr}= total area of transverse reinforcement within the spacing, s, that crosses the plane of splitting through the reinforcement being developed (mm^2).

s = maximum spacing of transverse reinforcement within L_d, center-to-center.

n = number of bars or wires being developed along the plane of splitting.

d_{cs}= spacing or cover dimension.

The development length, L_d, may be multiplied by the factor ($A_{s\ required}$) / ($A_{s\ provided}$) where reinforcement in a flexural member exceeds that required by analysis, except where anchorage or development for f_y is specifically required or the reinforcement is designed.

2.2.4 Lap Splices

A lap splice joint transfers the force from one bar to another through the concrete surrounding both bars. At any point along a splice, forces are being transferred from one bar by bond to the surrounding concrete and simultaneously, also by bond, to the other bar of the pair forming the splice. Within concrete, these forces can generate high shear stresses as well as splitting forces. The integrity of a lapped splice depends on the development of adequate bond along the surfaces of the two bars and on the ability of the concrete around the two bars transfer shear without disintegration or excessive deformation. The danger of concrete splitting is particularly great in the vicinity of tension splices. Two spliced bars generate diagonal compression in the space between them, and a clamping force is required to prevent a possible separation. The wedging effect of each of the two spliced bars may lead to a splitting crack along a line passing through the centers of lapped bars. Moreover, the interaction of ring-tension stresses around the bars creates an oval shaped tensile zone. Figure (2-7) shows the zone of ring tension stresses and the common splitting crack patterns. Hamad and Mansour (1996) [14] showed an optimal lap spacing of 5 d_b where a 7 -10% increase in bond strength over contact splices was observed. Beyond 5 d_b, the bond strength dropped off below the contact splice bond strength. Their tests were for lap lengths of 17 to 20 d_b without confinement.

2.2.5 Confinement of Spliced bars

The splitting strength of concrete can be enhanced if compressive stresses are superimposed onto the tensile-ring stresses around the lap splice zone. The concrete is said to be “confined” when compressive forces are used to counteract internal splitting forces. Spirals, transverse ties, and stirrups in anchorage zones are examples of confinement. Such confinement systems do not begin to counteract splitting forces until radial cracks starting from the bar surface the axis of the confining towards reinforcement as shown in Fig. (2-8). Because confining steel dose not play any part in resisting tensile splitting stresses until the splitting cracks intersect the confinement, they are termed a passive confinement. The splitting resisted by confining reinforcement is dependent on the width of splitting cracks, which taper along their length from the bar being developed as shown in Fig. (2-9). Thus, the confining reinforcement is more effective when it is placed close to the surface of a bar.

Many experimental studies have been performed on passive confinement. The results of those studies have been incorporated into the development length modification factors found in structural concrete design codes . In general, stirrups or transverse reinforcements, placed so that it intersects splitting crack planes, helps to improve bond capacity if splitting failure modes control. Beyond a certain level, pullout failure modes begin to determine the bond capacity and increasing confining steel fails to improve bond capacity in this case.

2.2.6 Lap splice in different building Codes

2.2.6.1 Egyptian code 203-2007[9]

According to the Egyptian code:

a. The spliced bars may be contact or non–contact. The distance between non-contacted bars should not exceed 150 mm or one fifth of the lap splice length whichever less, as shown in Fig. (2-10).

b. For members subjected to flexure, it is recommended to splice the tension bars in a staggered pattern in the longitudinal direction, as shown in Fig. (2-11). The distance between the centerlines of the laps is equal to at least 1.3 times the lap splice length, as shown in Fig. (2-11).
c. The lap splice length shall not be less than the development length; L_d, on condition that the area of steel in the section; $A_{s\ (applied)}$, is greater or equal to the required steel area; $A_{s\ (required)}$, and the percentage of lapped steel shall not exceed 25% of the total steel area at section.
d. If the percentage of lapped bars may exceed 25%, or the area of steel in the section is lesser than twice the required area, and the lap splice length is taken as 1.3 the development length (L_d), as shown in Fig. (2-11).
e. The percentage of lapped bars in compression may be taken as 100% of the steel area at a section with a lap length equal to L_d in compression
f. For members subjected to axial tension, lap splices are not allowed. However, bars maybe spliced by welding or by mechanical connection. The splice should be staggered with the distance between the centerlines of the splice not exceeding to 750 mm.
g. Lap splices are not allowed for bars with a diameter more than 28 mm. such bars are spliced by welding or by using mechanical connections.
h. When the splice contains several bar diameters, the lap splice length is obtained using the greatest bar diameter.

2.2.6.2 ACI 318-14[2]

a. Lap splices shall not be used for bars with diameter larger than 36 mm.
b. Bars spliced by noncontact lap splices in flexural members shall not be spaced transversely farther apart than the smaller of one-fifth the required lap splice length, and 150 mm.
c. Lap splices of deformed bars and deformed wire in tension shall be Class B splices except that Class A splices are allowed when: (a) the area of reinforcement provided is at least twice that required by analysis over the entire length of the splice; and (b) one-half or less of the total reinforcement is spliced within the required lap length.
d. Minimum length of lap for tension lap splices shall be as required for Class A or B splice which are defined in Table 2-2, but not less than 300 mm, where:
Class A splice..... 1.0 L_d

Class B splice..... 1.3 L_d

Where L_d is the tensile development length can be calculated by equation (2-3).

e. Splices shall be staggered at least 600 mm as shown in Fig. (2-12), and in such manner as to develop at every section at least, twice the calculated tensile force at that section but not less than 140 N/mm^2 for total area of reinforcement provided.
f. In computing the tensile forces that can be developed at each section, the spliced reinforcement stress shall be taken as the specified splice strength, but not greater than f_y. The stress in the un-spliced reinforcement shall be taken as f_y times the ratio of the shortest length embedded beyond the section to L_d, but not greater than f_y.

2.2.6.3 Eurocode 2-2004[10]

a. The following conditions must be considered when lap splice joints are conducted;

   1- The transmission of the forces from one bar to the next is assured,
   2- Spalling of the concrete in the neighborhood of the joints does not occur,
   3- Large cracks, which affect the performance of the structure, do not occur.

b. Laps between bars should be staggered and not located in areas of high stress.
c. Laps at any section should be arranged symmetrically.
d. The arrangement of lapped bars should comply with the conditions illustrated in Fig. (2-13):
   1- The clear transverse distance between two lapped bars should not be greater than 4 d_b or 50 mm, otherwise the lap length should be increased by a length equal to the clear space exceeding 4 d_b or 50 mm.
   2- The longitudinal distance between two adjacent laps should not be less than 0.3 times the lap length, L_o.
   3- In the case of adjacent laps, the clear distance between adjacent bars should not be less than 2 d_b or 20 mm.
e. When the provisions comply with conditions mentioned in point (d) above, the bars are all in one layer. Where the bars are in several layers, the percentage should be reduced to 50%.
f. All bars in compression and secondary (distribution) reinforcement may be lapped in one section.
g. The design lap length can be calculated from the following equation;

$$L_o = \alpha_1\,\alpha_2\,\alpha_3\,\alpha_5\,\alpha_6\,L_d \geq L_{o,\,min} \quad \text{..... (2-8)}$$

Where;

α_1 = coefficient represents the effect of the form of the bars assuming adequate cover.

α_2 = coefficient represents the effect of concrete cover.

α_3 = coefficient represents the effect of confinement by transverse reinforcement.

α_5 = coefficient represents the effect of the pressure transverse to the plane of splitting along the design anchorage length.

$\alpha_6 = (\rho_1/25)^{0.50}$ but not exceeding 1.5, where ρ_1 is the percentage of reinforcement lapped within 0.65 L_o from the center of the lap length considered.

L_d is the development length can be calculated by equation (2-5), and the minimum lap length ($L_{o,\,min}$) > max of $\{0.3\alpha_6 L_{d;}\ 15\ d_{b;}\ 200\ mm\}$.

h. Transverse reinforcements are required in the lap zone to resist transverse tension force.
i. When the diameter d_b of the lapped bars is less than 20 mm, or the percentage of the lapped bars in any section is less than 25%, then any transverse reinforcement or links necessary for other reasons may be assumed sufficient for the transverse tensile forces without further justifications.
j. When the diameter d_b of the lapped bars is greater than or equal to 20 mm, the transverse reinforcement should have a total area, A_{st} (sum of all legs parallel to the

layer of the spliced reinforcement) of not less than the area A_s of one spliced bar ($\Sigma A_{st} \geq A_s$). It should be placed perpendicular to the direction of the lapped reinforcement and between that and the surface of the concrete.

k. If more than 50% of the reinforcement is lapped at one point and the distance, (a), between adjacent laps at a section is $\leq$ 10 d_b as shown in Fig. (2-13) transverse bars should be formed by links or U bars anchored into the body of the section.

l. The transverse reinforcement provided for (j) above should be positioned at the outer sections of the lap as shown in Fig. (2-14).

2.2.6.4 Canadian code CSA A23.3-04 [7]

a. Lap splices shall not be used for bars with diameter larger than 35 mm.

b. Bars spliced by lap splices in flexural members shall have a transverse spacing not exceeding the lesser of one-fifth of the required lap splice length or 150 mm.

c. Lap splices of deformed bars and deformed wire in tension shall be Class B splices, except that Class A splices shall be permitted given the following condition are:
   1. The area of reinforcement provided is at least twice that required by analysis at the splice location.
   2. Less than one-half of the total reinforcement is spliced within the required lap length.

d. The minimum length of lap for tension lap splices shall be as required for a Class A or B splice, but not less than 300 mm, where
   1. The Class A splice length is 1.0 L_d.
   2. The Class B splice length is 1.3 L_d.

   Where L_d is the tensile development length can be calculated by equation (2-6).

e. Splices shall be staggered by at least 600 mm and in such a manner as to develop, at every section, at least twice the factored tensile force at that section, but not less than 140 MPa for the total area of reinforcement provided.

e. In computing the tensile resistance developed at each section, spliced reinforcement shall be rated at the specified splice strength. Unspliced reinforcement shall be rated at that fraction of f_y defined by the ratio of the shorter actual development length to the development length, L_d, required to develop the specified yield strength, f_y.

Table 2-1 gives a summary for the requirements recommended by building Codes for lap splices. Table 2-1 indicates that:

1- According to all Codes, the lap splice length; L_s or L_o, is considered as a factor of the development length L_d. The development length is a function of bar diameter d_b, steel yield strength f_y, and the square root of concrete strength $\sqrt{f_c'}$, then modify the development length to get the lap length.

2- The Egyptian Code modifies the basic development length considering bar ends, bar location, bar surface, and the percentage of provided reinforcement to the required reinforcement. While other Codes take more variables into consideration, such as the percentage of cut off ratio, the number of layers, the type of concrete, the transverse distance between bars, the cover distance, and the existence of transverse reinforcement like stirrups.

3- Most of the previous discussed codes allow 100% cut off ratio along the lap splice length, while Eurocode 2-2004, add a condition that if the longitudinal reinforcement arranged in several layers or the splice joints are not staggered, the percentage should be reduced to 50%.
4- The Egyptian Code 203-2007 permits more than 25% cut off ratio at the same section, if the provided lap splice length is taken as 1.3 the development length(L_d),while both the Eurocode 2-2004, ACI 318-14, and CSA 23.3-04 permit 50% cut off ratio.
5- In the Egyptian Code 203-2007, ACI 318-14, and CSA 23.3-04, the clear distance between bars in one layer shall not exceed one-fifth the required lap splice length, or 150 mm, while the Eurocode 2-2004 does not permit a distance less than 4 times the bar diameter.
6- Egyptian Code 203-2007, and Eurocode 2-2004 recommend that the staggering distance shall not be less than 1.3 times the lap splice length, while splices shall be staggered at least 600 mm according to ACI 318-14, and CSA 23.3-04
7- Only Egyptian Code 203-2007, among the previously studied codes, prevents using lap splice in section subjected to direct tension.
8- Egyptian Code 203-2007 prevents the usage of lap splice, if the bar diameter is greater than 28 mm, while ACI 318-14, and CSA 23.3-04 prevented the usage of lap splice, if the bar diameter is greater than 36 mm, and 35 mm respectively.

All the calculated values using Egyptian Code 203-2007, ACI 318-14, Eurocode 2-2004, and CSA 23.3-04 are given in Table 2-3. From Table 2-3, it is obvious that, the lowest allowed lap splice length is recommended by Eurocode 2-2004 as 37 times the bar diameter.

2.3 Previous Experimental Work on conventional lap splices without head

Ferguson, et al. (1965) [11] studied 35 reinforced concrete beams, to study the effect of bar diameter, stirrups, and concrete strength. All beams were with bars placed in the bottom of the beam, 21 beams with 25 mm bars and 14 beams with 35 mm bars. Some of these beams were without stirrups. Longitudinal and cross-sectional details of the beam specimens are shown in Fig. (2-15). They concluded that stirrups increased splice strength, minimum stirrups as much as 20%, and heavy stirrups up to 50%. The splitting prior to failure gradually developed over the full splice lengths seemed almost to stabilize with a substantial center length remaining un-split until a final catastrophic failure occurred.

Hamad, et al. (1996) [14] performed experimental work on seventeen full-scale slab specimens to obtain a more complete understanding of the effect of bar spacing of a tension lap splice on the bond strength of splices failing by splitting. Each slab was reinforced with three lap splices, and was designed to fail by bond splitting. The splice length of the deformed bars was selected to develop a steel stress less than yield to ensure the occurrence of a splitting mode of failure in all slab specimens. A yielding mode of failure provides little or no

information regarding bond strength of a reinforcing bar, and the objective was to compare relative bond behavior of non-contact lap splices. The splice length was set at 300 mm for slabs reinforced with bars 14 and 16 mm in diameter, and 350 mm for the 20 mm bar specimens. A 20 mm concrete cover to the reinforcing bars in the splice region was chosen as a typical side and bottom cover (19.1 mm) as specified by the ACI Code. Longitudinal and cross-sectional details of the slab specimens are shown in Fig. (2-16). Slabs reinforced with bars 20 mm in diameter required transverse reinforcement in the shear spans to avoid shear failure. They concluded that:

1- For slabs with contact lap splices or small clear splice-bar spacing (10 percent of the lap splice length; L_o), the final cracking pattern on the side faces of the splice region was more or less confined to the level of the reinforcement. Also, longitudinal splitting cracks on the bottom tension face developed along the splices. As the spacing of splice-bar, was increased, flexural cracks on the side faces of the splice region were inclined at a larger angle from the horizontal and had higher propagation along the slab height. Also, diagonal surface cracking of concrete between the splice bars became more prominent.

2-The ultimate load resisted by the slab specimens varied with spacing between lapped bars. The optimum clear splice-bar spacing was 4.3 d_b (20 percent of L_o) for slabs reinforced with bars 14 mm in diameter, 5.6 d_b(30 percent of L_o) for the 16 mm bar specimens, and 5.3 d_b (30 percent of L_o) for the 20 mm bar specimens.

3- For the three bar sizes studied, bond strength of non-contact splices increased relative to the contact splices up to an optimum clear splice-bar spacing of 30 percent of the splice length. At this spacing, bond ratios (non-contact to contact splices) were 1.06 for the 14 mm bars, 1.09 for the 16 mm bars, and 1.10 for the 20 mm bars.

4- When the measured bond stresses of splices were compared with the theoretical values computed using the 1989 ACI Building Code (ACI 318-89) bond provisions, it was found that the ACI 318-89 bond specifications are highly conservative and should be modified to provide a better and more reasonable estimate of the bond strength of bar splices in slab specimens. Based on this study, it can be concluded that the ACI limit concerning the transverse spacing of non-contact tensile lap splices of 20 percent of the lap length is conservative. A limit of 30 percent of splice length is recommended. It would be even more appropriate from a designer point of view to set the limit in terms of bar diameter. Within the scope of their study, spaced-bar splices developed greater bond strength than contact-bar splices up to an optimum clear spacing of around five times the bar diameter (5 d_b) .

Hamad, et al. (2003) [13] conducted twelve full-scale beam specimens. The main studied variables were the bar size, concrete strength, number of splices, and c/d_b ratio (i.e. the ratio between the smaller of the distance from center of bar to nearest concrete surface or 1/2 of center-to-center spacing of bars being developed and the bar diameter). The role of concrete compressive strength was assessed by testing normal- and high strength concrete specimens with nominal compressive strength values of 28 and 60 N/mm^2, respectively. For each level of concrete strength, a series of six specimens was tested. In each series and for each of three bar sizes: 20, 25, and 32 mm, two identical companion beams, except for whether the bars were black or galvanized, were tested. Each beam was reinforced on the tension side with reinforcing bars spliced at mid-span in a constant moment region. Longitudinal and cross section details for the beams with different bar sizes are shown in Fig. (2-17).The mode of failure was splitting of the concrete cover in the splice region. The effect of galvanizing was evaluated by comparing the mode of failure, load-deflection curves, and

average bond strength values. In the Normal Strength Concrete (NSC) series, there was a slight reduction in the ultimate strength value of galvanized bar beams as compared with their companion black bar beams. The reduction in bond strength due to galvanizing ranged from 4 to 6%. In the HSC series, however, the reduction in bond strength due to galvanizing was substantially more ranging from 16 to 25%.

Tarabia, et al. (2010) [21] conducted experimental tests on twelve simply supported concrete beams to study the behavior of lap splice of steel reinforcement in tension zone. The main objectives of this experimental program were: (a) - To study the behavior of reinforced concrete simply supported beams with lap splice of tension steel reinforcement zones with different lap splice lengths and arrangements. (b)- To obtain a spliced beam that can achieve at least the same strength and ductility of the same beam without any splices using transverse reinforcement with different shapes. (c)- To investigate the old condition of the Egyptian code, which was removed from the last version of the code (2007), which is not to splice more than one quarter of tension steel at the same section. The dimensions of beams were 150 mm × 260 mm × 2600 mm. All the specimens had the same concrete strength, and four 10 mm-diameter 400/600 high strength steel were used as tension reinforcement. Plain bars of 6 and 8 mm diameter agree with grade 280/450 were used for stirrups outside the splice zone and top reinforcement respectively. The main studied variables were: cut-off ratio, lap splices length, the type, spacing, and shape of transverse reinforcement at the splice zone. Figure (2-18) shows the longitudinal and cross-sectional details of the some beam specimens. From the results of the studied beams, they concluded that:
For the same value of the lap splice length as that recommended by Egyptian Code, without the use of transverse reinforcement at the spliced zone, the change of the cut off ratio from 25% to 100% resulted in a reduction in ductility. On the other hand, there was a drastic increase in ductility of beams when transverse reinforcement was used.

Abdel-Kareem, et al. (2013)[1] conducted experimental testes on seventeen simply supported concrete beams to study the effect of transverse reinforcement on the behavior of lap splice of steel reinforcement in tension zones in high strength concrete beams. The cross section dimensions of tested beams were 160 x 250 mm, and the concrete cover was constant in all sides of beams and equal to the spliced bar diameter (d_b), with a distance of 3000 mm between the supports. Reinforcement on the tension side consisted of two 16 mm diameter deformed bars spliced at mid-span. Plain bars of 8 mm diameter agree with grade 280/450 were used for stirrups outside the splice zone. Longitudinal and cross section details of the beam specimens are shown in Fig. (2-19).The shapes of stirrups around spliced bar are shown in Fig. (2-20).The parameters included in the experimental program were the concrete compressive strength, the lap splice length, the amount of transverse reinforcement provided within the splice region, and the shape of transverse reinforcement around spliced bars.
From these tests, they concluded that:
The displacement ductility increased and the mode of failure changed from splitting bond failure to flexural failure when the amount of transverse reinforcement in splice region increased, and the compressive strength increased up to 100 MPa. The presence of transverse reinforcement around spliced bars had pronounced effect on increasing the ultimate load, the ultimate deflection, and the displacement ductility.

2.4 Headed bars

Headed bars are manufactured by attaching a plate or nut to the end of a reinforcing bar to provide a large bearing area that can help to anchor the tensile force in the bar. Figure (2-21) shows an example of a headed bar. The tensile force in the bar can be anchored by a combination of bearing on the ribs of the bar sides and on the head. Many researches have suggested that using headed bars may provide a better solution than conventional straight bar for some splicing applications.

2.5 Mechanism of Headed Bars

ACI 318-2014[2] commentary describes two mechanisms of headed reinforcement bars. The first "development of headed bars" describes cases in which the force in the bar is transferred to the concrete through a combination of a bearing force at the head and bond forces along the bar, while the second mechanism "anchorage" describes cases in which the force in the bar is transferred through bearing to the concrete at the head alone.

2.6 Development Length of Headed Deformed Bars in Tension

2.6.1 ACI 318-2014 development length [2]

a. Development length for headed deformed bars in tension, " L_{dt}", shall be determined from Equation (2-9). Use of heads to develop deformed bars in tension shall be limited to conditions satisfying (1) through (6):
   1. Bar yield stress, f_y shall not exceed 420 MPa.
   2. Bar size shall not exceed 36 mm.
   3. Concrete shall be normal weight.
   4. Net bearing area of head A_{brg} shall not be less than 4 A_b, where, A_b = nominal bar area.
   5. Clear cover for bar shall not be less than 2 d_b, where, d_b = bar diameter.
   6. Clear spacing between bars shall not be less than 4 d_b.

b. For headed deformed bars satisfying the previous conditions ACI 318-2014, development length in tension L_{dt} shall be

$$L_{dt} = \left(\frac{0.19\,\Psi_e\, f_y}{\sqrt{f_c'}} \right) d_b \quad \text{..... (2-9)}$$

Where:
f_c' = cylinder compressive strength of concrete, MPa, The value of f_c' used to calculate L_{dt} shall not exceed 40 MPa, fy = yield stress of reinforcement in MPa, Ψ_e = factor used to modify development length based on reinforcement coating (taken as 1.2 for epoxy-coated reinforcement and 1.0 for other cases).

c. Where reinforcement provided is in excess of that required by analysis, except where development of f_y is specifically required, a factor of ($A_{s\ required}$ / $A_{s\ provided}$) may be applied to the expression for "L_{dt}".
d. Length "L_{dt}" shall not be less than the larger of 8 d_b and 150 mm.
e. Heads shall not be considered effective in developing bars in compression.

f. Any mechanical attachment or device capable of developing f_y of reinforcement is allowed, provided that test results showing the adequacy of such attachment or device are approved by the building official. Development of reinforcement shall be permitted to consist of a combination of mechanical anchorage plus additional embedment length of reinforcement between the critical section and the mechanical attachment or device.

2.6.2 According to CSA A23.3-04[7]

The Canadian Code has provided the following conditions:

a. Crossties shall be anchored by standard tie hooks or by heads of headed bars.
b. Headed bars and studs with a head of an area equal to ten times the bar area (equal two times the head area recommended by ACI 318-2014), shall be deemed capable of developing the tensile strength of the bar without crushing of the concrete under the head provided that the specified concrete compressive strength is equal to or greater than 25 MPa and the yield strength of the bar used in the design does not exceed 500 MPa.
c. Any mechanical anchorage, including heads of headed bars or headed studs, demonstrated by test to be capable of developing the strength of reinforcement without damage to the concrete, may be used.
d. The development of reinforcement may consist of a combination of mechanical anchorage and additional embedment length of reinforcement between the point of maximum bar stress and the mechanical anchorage.
No equation has been provided by this code.

2.7 Types of Headed Bars

This section discusses the products of the three main types of headed bar fabricated by: friction-welding plates on the ends of bars, forging heads on the ends of bars using portable devices, and using threaded heads with threading the bars . Heads can be fabricated in a variety of shapes such as square, rectangular, and circular.

2.7.1 Friction-welded Heads [22]

The friction-welded heads are manufactured by pressing the end of a deformed reinforcing bar onto a plate spinning at very high speed. The heat produced by the friction between the deformed bar and plate causes the bar material to melt and form a weld between the two members. The machinery required for this process is quite large and the headed bars can only be created in factory conditions. The headed bars made with four shapes: square, rectangular, and circular. Figure (2-22) shows a typical of friction-welded head.

2.7.2 Forged Heads [17]

The forged head on the ends of bars using portable devices, the forged head is shown in Fig. (2-23). First the bar end is preheated with a blowtorch, and then a special hydraulic device is used to forge the head out of the material of the bar.

2.7.3 Threaded Heads [22]

This type is manufactured by tapered thread connection between the reinforcing bar and a special nut that is screwed onto the bar to provide a head. Figure (2-24) shows this type.

2.8 Previous Research on Headed Bars

The available research on headed bars can be separated into two categories: application studies and general behavior studies. The distinction between the two categories derives from the scope of the research. The research grouped under application studies tends to focus on a particular structural of headed bars usage. General behavior studies are those research programs aims at determining mode of behavior that can extrapolated to many different types of structural situations.

2.8.1 General behavior studies

Some of the researches deemed to study general behavioral trends are reviewed within this section.

Nineteen pullout tests of headed bars were conducted at the Transportation Laboratory of the California Department of Transportation (Caltrans) in the early 1970's [20].
Their test specimens used large diameter reinforcing bars with #11, #14, and #18 (36 mm, 43 mm, and 57 mm) sizes. The purpose of the tests was to determine if headed bars could represent a viable alternative to hooks in monolithic bridge pier/superstructure connections. The scope of the study also involved testing of several different head-bar connections. The various connections are shown in Fig. (2-25). With only two exceptions, the headed bars tested used very large head sizes: relative head areas of 15.0 for the #11 (36 mm) and #14 (43 mm) bars tested and 13.1 for the #18 (57 mm) bars tested. The two exceptions included one non headed #18 (57 mm) bar and one small headed #18 (57 mm) bar using only a cad-weld coupler sleeve as anchorage (the sleeve provided a relative head area of 1.8). The test specimens consisted of tensile pullout specimens similar to those shown in Fig. (2-26). Large embedment lengths were provided for the bars. Additionally, supplementary transverse reinforcement was used around the perimeter of the specimen blocks. The variables tested included: bar size (#11, #14, or #18) (36 mm, 43 mm, or 57 mm), single versus group action (four bar groups of #11's) (57 mm's), concrete cover (7 1/2" or 19") (191 mm or 483 mm), and embedment depth (h_d/d_b = 8 to 32).
It was realized that the bonded lengths of the bars were too long to allow much anchorage capacity of the bars to be carried by the heads. In most tests, the test bar yielded in tension or the load to failure exceeded the capacity of the test frame. This research provided the following conclusions:
1- The head sizes selected for testing were more than adequate for the development lengths tested in the research program.
2- One test of a much smaller head size (A_{nh}/A_b = 1.8) provided comparable results to similar tests of larger head sizes (A_{nh}/A_b = 13) indicating that smaller head sizes could achieve yield. Also, smaller heads should be investigated in any forthcoming research.
3- More load was carried by the head as the bonded length of the bar was reduced.
4- Load-slip measurements of the tested bars indicated that more slip is experienced for bars acting in groups than single headed bars.

Devries (1996) [8] tested over 140 pullout testes to determine the effects of several variables on the anchorage of headed bars in concrete. The main studied variables included: Clear cover, corner placement, close spacing, concrete strength, embedment depth, development length, transverse reinforcement, bar diameter, head size, head shape, and head thickness. The concrete used was of nominal strengths 21 to 69 MPa, three reinforcement bar sizes (20, 25, and 35 mm diameter) and large relative headed bars area (5.7 and 7.4). Devries divided the tests in two groups: shallow embedment tests and deep embedment tests. The shallow embedment setup consisted of a headed bar with a ratio of embedment depth to clear cover less than five. Figure (2-27) shows shallow embedment pullout specimen used by Devries. The deep embedment setup consisted of a headed bar with a ratio of embedment depth to clear cover larger than five. Figure (2-28) shows deep embedment pullout specimen used by Devries. The testes led to the following conclusions. For the shallow embedment, it was concluded that:

1- The anchorage capacity enhanced by increasing embedment depth, edge distance and concrete strength.

2- For bars with low ratios of embedment depth to edge distance, pullout –cone failure and bar failure were the two modes controlling the anchorage capacity.

3- Development length added strength to anchorage but it is conservative to ignore this increase.

4- Transverse reinforcement placed perpendicular to the headed bars had no effect on the anchorage capacity or behavior.

5- Bar placement near one edge reduced the anchorage capacity compared to placement away from all edges and corner placement reduced the capacity further.

6- The design equation for pullout – cone capacity of a headed reinforcing bar (in SI units) is:

$$P_u = \Psi \frac{A_n}{A_{no}} \frac{h_d^{1.5}\sqrt{f_c'}}{112} \leq \frac{A_b f_y}{1000} \leq \frac{A_b f_u}{1000} \quad \text{..... (2-10)}$$

$$\Psi = 0.70+0.30 \frac{C_1}{1.5\, h_d} \leq 1.0 \quad \text{..... (2.11)}$$

where P_u is the anchorage capacity in kN, h_d the embedment depth in mm and f_c' the concrete compressive strength in MPa. A_n is the available failure surface for a single bar or group of bars based on the perimeter of the heads as shown in Fig. (2-29) and A_{no} the basic failure surface area equal to 9 h_d^2. The value Ψ takes into account the disturbance of radial stress for placements near edges and calculated by Equation (2-11). C_1 is the minimum edge distance, A_b being the bar area in mm^2, f_y the yield stress and f_u the ultimate bar stress in MPa.

For the deep embedment, it was concluded that:

1- The primary factors affecting the blowout capacity of the anchorage were the edge distance, net bearing area of the head and concrete compressive strength.

2- For bars with large ratios of embedment depth to edge distance, side blowout failure and bar failure were the two modes controlling the anchorage capacity.

3- Development length increased the anchorage capacity but again it is conservative to ignore this increase in strength.

4- Transverse reinforcement in the anchorage zone did not increase the ultimate capacity though large amounts of transverse reinforcement placed near the head did increase the level of load maintained after the initial blowout failure.
5- Corner placement and close spacing of bars reduced the blowout capacity of headed reinforcement.
6- The design equation for the blowout capacity of a headed reinforcement bar (in SI units) is:

$$P_u = \Psi \frac{A_{bo}}{A_{bon}} \frac{c_1\sqrt{A_n f_c'}}{80} \leq A_{bf_y} \leq A_{bf_u} \quad \text{..... (2-12)}$$

$$\Psi = 0.70+0.30\frac{c_2}{3c_1} \leq 1.0 \quad \text{..... (2.13)}$$

where P_u is the blowout capacity in kN, c_1 the minimum edge distance in mm, A_n the net bearing area of the head in mm^2, and f_c' the concrete compressive strength in MPa. The ratio A_{bo} over A_{bon} is the ratio of available failure area for single bar or group of bars and the basic failure area. A_{bo} equals to 36 C_1 as shown in Fig. (2-30). The value takes into account the disturbance of radial stress by corner placement and calculated by Equation (2-13). C_2 is the minimum orthogonal edge distance, A_b being the bar area in mm^2, f_y the yield stress and f_u the ultimate bar stress in MPa. The design equations for both the blowout and pullout-cone modes of failure assume the head is adequately stiff. Based on the obtained tests results, the head should be design to prevent yielding of the head in bending under a uniform distribution of bearing stress at the ultimate load.

Bashandy (1996) [3] carried out a study to determine the anchorage behavior of headed bars in joints. The study was divided into three phases: Basic studies on headed bars, anchorage in exterior joints, and effects of seismic (cyclic) loading.
Fourteen pullout tests on bars embedded in concrete cubes were conducted to investigate the effects of cyclic loading and anchoring the head behind a crossing bar on the anchorage behavior and capacity of headed bars. Figure (2-31) shows test setup for pullout tests. The variables included number of load cycles, size of crossing bars, and head dimensions. The following conclusions were made concerning the variables investigated:

1- Cycling the load between 5 and 80% of the ultimate capacity, up to 15 cycles, did not significantly influence the anchorage capacity of headed bars.
2- The increase in slip due to load cycling was dependent on the maximum load of each cycle.
3- Placing a crossing bar in the anchorage zone of the head improved the anchorage capacity through two mechanisms. First, the crossing bar provided a lateral restraint against side blowout by mobilizing more concrete to resist spalling failure. Second, the crossing bar increased the effective bearing area of the head, which led to lower bearing stresses.
4- Although the increase in anchorage capacity rose with an increase in diameter of the crossing bar, it was conservative to limit this increase for design purposes to 25% for heads positively anchored behind 25 mm or larger crossing bars. A positive anchorage means that the clear head dimension is at least equal to half the crossing bar diameter.

Thirty-two large-scale specimens' simulating of exterior joints in a structure were tested to assess the effects of different variables on the behavior of joints under monotonic loading. Figure (2-32) shows concrete dimensions and reinforcement details of the headed bar specimen. The variables included size of anchored bars, head dimensions and orientation,

embedment length, concrete cover, and confining reinforcement. The following observations and conclusions were made concerning the behavior of head bars in exterior joints:

1- The bar load was transferred to concrete through two mechanisms: anchorage along the embedment length, and bearing of the head on concrete. In most cases, the first mechanism was not effective in increasing the ultimate load because large slip at failure caused bond deterioration along the lead embedment.
2- Although anchorage along the bar embedment increased the ultimate load in few cases, the contribution of the two mechanisms should be considered as a unit because both are affected by the lead embedment length.
3- Head aspect ratio and orientation do not have significant effect on the anchorage capacity of headed bars.
4- Bar diameter does not have significant effect on the anchorage capacity of the load-slip behavior of headed bars.
5- The anchorage capacity increased with the increase of side concrete cover. Increased side cover provides a larger mass of concrete to resist side blowout.
6- Confining reinforcement improved concrete bearing capacity under the head and increased the ultimate load. Both slip and load drop at failure were significantly lower in specimen with confining reinforcement.
7- The anchorage capacity of headed bars as obtained from pullout tests was significantly higher than that obtained from exterior joint tests. The difference in capacity is attributed to joint shear cracking before anchorage failure.
8- The proposed design Equation (2-14) for the development length required to develop yield stress in a headed bar terminating in an exterior joint is

$$l_d = \frac{A_b f_y}{14.7\,\alpha\beta\gamma \sqrt[3]{A_n}\sqrt{f'_c}} + d' \qquad \text{(2-14)}$$

where l_d = required embedment length, in mm, A_b = area of the anchored bar, in mm^2, f_y = yield stress of the anchored bar, d' = distance from the face of the column to centroid of the column longitudinal reinforcement closest to face, in mm, A_n = net bearing area, in mm^2, α = confining reinforcement factor, taken as 1 for tie spacing more than 100 mm, 1.25 for spacing equal to 100 mm to 51 mm, and 1.4 for tie spacing equal to 50 mm or less, β = cover size factor, taken as 0.8 for side cover less than 76 mm, and 1 for all other cases, γ = anchorage condition factor, taken as 1.25 for heads positively anchored behind 25 mm or larger crossing bars, and 1 for all other anchorage conditions.
The embedment length required by this equation for a bar with a head is equal to 8 times the bar area which is 30% less than that required by ACI Building Code for a bar terminating in a standard hook.

One exterior beam-column subassemblage was tested under cyclic loading to provide an insight to potential benefits of replacing hooked bars by headed bars in seismic areas. Figure (2-33) shows test setup for this exterior joint. The behavior of the specimen was compared with a similar specimen constructed using hooked bars, which was reported by Bashandy [3].
The overall behavior of the headed bar specimen was superior to that of the hooked bar specimen. Capacity degradation was minimal, and no signs of bond deterioration were observed. The test ended after the column section was damaged and its longitudinal bars were yielded.

Ledesma (2000) [17] tested sixteen slab tests to determine the behavior of unconfined headed bar lap splices. The variables included strength of staggered splices versus adjacent splices, head size, head shape, bar spacing, lap length, and bar size. All of the specimens had the same basic dimensions were 4.0 m in length and had a nominal depth of 250 mm but varied in width. The width of the specimens was 1000 mm, 900 mm and 625 mm. Center-to center bar spacing of the lapped bars (S_{bar}) was either 150 mm or 250 mm ($6d_b$ or $10d_b$) as shown in Fig. (2-34). Bar sizes used in this study were 16 mm's and 25 mm's. Figure (2-35) shows typical reinforcing layouts for the test specimens. The tested specimens were reinforced with transverse reinforcement outside of the constant moment region containing the lap splice zone. Clear cover over the heads was at least 34 mm. The following observations and conclusions were made concerning the behavior of headed bars in lap splices:

1- Staggered lap splices did not perform as well as adjacent lap splices. Staggered splices were spaced so that all bars were equal distances from each other and adjacent splices were spaced so that spliced bars were as close as the heads would permit.
2- Capacity increased as head size was increased. However, the effect that head size had on capacity diminished as lap length increased due to increased force transfer by bearing of the lugs of the bar on the surrounding concrete. Head size was defined as the ratio of net head area to bar area. A_n/A_b ratios tested were 1.5 or 11.9 for specimens reinforced with d_b = 16 mm bars. A_n/A_b ratios ranged from 0.0 to 4.7 for specimens reinforced with d_b = 25 mm bars. The increase in capacity, due to head size, of specimens could be predicted using DeVries' model for side blowout capacity of headed reinforcement (Eq. 2-12) [8].
3- Head shape did not significantly affect the performance of the lap splices. Head shapes tested were square, rectangular, and circular.
4- Bar spacing did not seem to affect the performance of the lap splice tests. Bar spacing, s_{bar}, was either 150 or 250 mm.
5- Below a lap length of 5 d_b (the spacing between lapped bars), the mechanism of force transfer was entirely between the heads of the lapped bars and there was no contribution from bond to the lap capacity. Also, the capacity provided by the heads was less at the short (5 d_b or less) lap lengths.
6- The effect that bar size had on the development of headed bar splices was inconclusive because three of the four specimens reinforced with d_b = 16 mm bars failed by yielding of the reinforcement. Such failures indicate that the splice is fully effective but do not indicate whether a shorter lap length would have been equally effective. The fourth specimen failed after splitting cracks formed along an outer edge splice.

Thompson, et al. (2002) [24] tested twenty-seven lap splices specimens to develop the anchorage of multiple headed bars anchored within a single layer lap splice. Also, specimens with non-headed bars were tested. The main studied variables of the lap splice test program included the lap length, the head size and shape, the bar spacing, contact versus non-contact laps, and the presence of confinement in the lap zone. Figure (2-36) shows the test setup of the lap splice. The studied specimens consisted of 250 mm thick, 4.0 m long slabs. The primary tensile reinforcement was spliced at the mid-span of these specimens. Both confined and unconfined lap splices were tested. Figure (2-37) shows the basic reinforcement layout for an unconfined specimen. Center-to center bar spacing of the lapped bars was either 150 mm or 250 mm ($6d_b$ or $10d_b$). The width of the specimen was altered to accommodate the bar spacing: 625 mm for 150 mm spacing and 900 mm for 250 mm spacing. Clear cover over the heads was at least 34 mm. In confinement specimens, as shown in Fig. (2-38), two

confinement details were studied; the first consisted of hairpin tie-downs at either end of the bars in the lap zone. In the second detail, transverse bars were placed over the lapped bars in the middle of the lap zone and connected to bars in the bottom of the beam using U-shaped ties with 90^o hooks. The testes led to the following conclusions:

1- The mechanism of stress transfer between opposing bars in non-contact lap splices was by struts acting at an angle to the direction of the bar. The resulting strut-and-tie mechanism caused the lapped bars were observed to occur at an angle of about 55^0 to the axis of the bar, as shown in Fig. (2-39). Lap length and bar spacing did not seem to effect this mechanism
2- The anchorage capacity of headed bars in lap splices was the same as headed bars in CCT nodes.
3- Data from the tests of this study indicated that the side cover dimensions should be taken as half the distance between opposing lapped bars.
4- Smaller bar spacing resulted in reduced head capacity.
5- Head size and shape did not affect the mechanism of stress transfer.
6- Deboning of the lapped bars eliminated bond-splitting cracks and increased the side cover dimension to the full center-to-center distance between opposing lapped bars. This eliminated the bond contribution to anchorage, but significantly improved the bearing capacity of the head due to the increase in side cover dimension.
7- Transverse confining bars parallel to the plane of the lap splice and placed within the concrete over the splices provided the best confinement for lapped bars.
8- Contact lap splices may have a greater capacity than non-contact lap splices, however, the only tests conducted with contact lap splices had very small lap lengths and anchorage lengths were less than $6d_b$. Additional tests on the effect of lap configuration should be conducted at longer lap lengths.

Thompson, et al. (2002[25], 2005[26], 2006[27]) tested Sixty-four compression - compression -Tension (CCT) node specimens to provide important experimental information on the behavior and failure modes of CCT nodes. Furthermore, the test results provide information on the anchorage behavior of headed reinforcement. The experimental data can be compared to several existing approaches for determining the capacity of nodes and anchorage capacity of headed reinforcement. A typical CCT node test is shown in Fig. (2-40).The critical CCT node is at the bottom left of the specimen. A detail of this node is provided in Fig. (2-41).The tie bar was either a single 25 or 36 mm bar. The width of the specimen was typically six tie bar diameters ($6d_b$). The bottom bearing plate was rigid and always full width, with a typical length of 4 d_b. The angle of the diagonal compression strut (θ_{strut}) was varied by changing the point of load application. Specimens were tested with 30, 45, and 55-degree strut angles. Typically, no secondary steel was placed near the node or along the length of the strut. However, some confined specimens with stirrups or special details in the node region were tested. The details of the stirrup-confined node specimens are shown in Figs. (2-42) and (2-43). The typical locations of strain gauges on the tie bar are shown in Fig. (2-41). In some specimens, additional strain gauges were placed on the tie bar or on confining stirrups or special reinforcement details within the diagonal strut and node zone as shown in Fig. (2-42).The testes led to the following conclusion:

For the behavior of CCT nodes, they concluded that:

1- The state of stress at a CCT node reversed on either side of the critical crack. Beneath the CCT node, compression stresses from the lower bearing plate necked inward to equilibrate spatially with the bearing face of the headed bar.
2- CCT nodes failed by mechanisms related to anchorage. Non headed bars failed by pullout from the node. Headed bars failed by explosive rupture at the node. Rupture was characterized by crushing just above the head and lateral splitting of the diagonal strut. The extent to which these two characteristics governed behavior depended on head size and orientation.
3- Variations in strut angle affected the anchorage length of the tie bar. Shallow strut angles increased the length of the extended nodal zone, moving the critical development point away from the head and increasing the contribution from bond to anchorage.
4- Stirrup confinement increased the anchorage length of the tie bar by changing the truss mechanism. Additionally, bond stress, ductility, and crack control were improved by the addition of stirrups.

For anchorage behavior of headed bars, they concluded that:

1- The anchorage of headed bars was mobilized in two stages. In the first stage, anchorage was carried almost entirely by bond stress, which peaked as the first stage ended. In the second stage, as bond began to deteriorate, bar stress was transferred to the head. Throughout the second stage, bond declined and head bearing increased. The second stage ended with yielding of the bar or bearing failure of the concrete at the head.
2- Bond stress at failure decreases as relative head area increases.
3- Slip of the head decreased as head size was increased. Slip occurred in two stages: insignificant head slip occurred before the head attained most of its capacity. Shortly before peak bearing capacity was reached, slip increased steadily until failure occurred.

For capacity of nodes, they concluded that:

CCT nodes anchored by headed reinforcement fail when bearing capacity at the head reaches a limit described by the following:

Bearing pressure, $\frac{N}{A_{nh}} = 0.9 f_c' (\frac{2C}{\sqrt{A_{nh}}}) \Psi$ ..... (2-15)

$$\Psi = 0.60 + 0.40 \frac{C_2}{C} \leq 2.0 \quad \text{.....(2-16)}$$

where N = bearing strength capacity, kN, A_{nh} = net head area, mm^2, c = minimum cover dimension, measured to bar center, mm, c_2 = minimum cover dimension, measured in direction orthogonal to c, mm, fc' = concrete compression strength, from cylinder tests, MPa, Ψ = radial disturbance factor.

Chun, et al. (2009) [6] tested thirty specimens simulating exterior beam-column joints with headed or hooked beam reinforcement anchorage, to investigate the concrete contribution to the anchorage strength, and no transverse reinforcement was placed in the joints. The specimens were designed to reflect the characteristics and boundary conditions of an interior CCT node typical of an exterior beam-column joint. The details of the specimens are presented in Figs. (2-45) and (2-46). The test setup examines the anchorage of

longitudinal beam reinforcement in an exterior beam-column joint using headed reinforcement. The embedment length" L_e" was varied from 8.4 d_b to 15.5d_b for d_b = 57 mm specimens and from 6.3 d_b to 10.4 d_b for d_b = 36 mm specimens and d_b = 25 mm specimens, where d_b denotes a bar diameter. The anchorage of a single longitudinal bar was examined to avoid interference of multi-bar effects. No transverse reinforcement was included to minimize potential confining enhancements to the anchorage. The studied variables included embedment length and bar diameter. Three bar diameters: 25, 36, and 57 mm were chosen, which represent a range of bars used for beam reinforcement. The width of the specimen is 6 times the headed bar diameter (6d_b). The clear side cover was 2.5d_b for a beam bar in an exterior joint. For comparison, two specimens with hooked bars were tested for each headed bar diameter examined. The embedment lengths for the hooked bar specimens were chosen to be equal to the longest and shortest embedment lengths of headed bars for each diameter. The head shape was circular with a net head area A_{nh}, equal to 4 times of the bar area A_b. The headed bars for the tests are shown in Fig. (2-44).The tests were terminated when the applied load decreased to 85% of the maximum load. The testes led to the following conclusions:

1- The head bearing strength contribution is proportional to the embedment depth normalized by the column depth.
2- The anchorage strength of the headed bars terminated within exterior joint with sufficient side cover (greater than 3 d_b from the bar center) can be accurately predicted by Equation (2-17).

$$P = n_{5\%}(P_{bearing} + P_{bond}) \quad \text{(2-17)}$$

$$= 0.78[(1+2.27\frac{l_e - 0.7D_c}{D_c})\ 0.85f_c'A_{nh} + 0.504\sqrt{f_c'}\ \phi_b(\ l_e - d_b\ )] \quad \text{(MPa)}$$

Where $\phi_b = \pi d_b$ is a bar perimeter, $n_{5\%}$ is a coefficient for 5% fractile (= 0.78 from statistical analysis), l_e and D_c as shown in Fig. (2-45).

Kang, et al. (2012) [16] tested two exterior beam-column connection subassemblies under cyclic lateral loading with closely spaced headed bars. The tests primarily explored the effect of using small clear spacing and multiple layers of headed bars in beams as shown in Fig. (2-47). All beams and columns were reinforced with a single type of headed reinforcement, and one end of each beam bar was anchored in the joint core. Headed deformed bars with a bar diameter of 19 mm were used. JH-R1 had a single layer for both the top and bottom beam bars, while JH-R2 had two layers for each of them as shown in Fig. (2-47). Consequently, the spacing between the headed bars was also different in the two specimens, the clear bar spacing was 2.1 d_b (horizontal) in JH-R1 and 1.3 d_b (vertical) in JH-R2, which was much smaller than the minimum limit of 4 d_b specified in ACI 318–08. The testes led to the following conclusions:

1- The specimens JH-R1 and JH-R2 exhibited ductile load-displacement behavior with beam hinging fully developed adjacent to the beam-joint interface, and no unfavorable mechanisms typically accompanying notable strength drops were found. .

2- Specimen JH-R2 with two layers of headed bars with heads touching each other showed a higher energy dissipation ratio as well as higher secant stiffness around zero drift than JH-R1 for the 4% drift cycle. This was likely because the closer horizontal spacing in JH-R1 slightly accelerated the bond deterioration of beam bars at the beam-joint interface and inside the joint, where all four beam bars were placed in a one layer near the top or bottom beam surface.
3- Based on the test results and previous test data, it was concluded that the clear bar spacing of approximately $2d_b$ or the use of two bar layers may be reasonably permitted for headed bars anchored in exterior RC beam-column joints subjected to earthquake-type loading.

Chun, and Lee (2013) [4] tested Twelve beams reinforced with lap spliced headed bars to investigate the anchorage behavior of high-strength headed reinforcement. Headed bars of Grade 600 MPa were used and the main studied variables included splice length (L_s), bar spacing/cover (c), bar diameter (d_b), concrete strength (f_c'), and transverse reinforcement contents (k_{tr}). A typical lap splice specimen is shown in Fig. (2-48). Two reinforcing bars were lapped at the midpoint of the specimen. Nine specimens were unconfined within the lap zone, and three confined specimens with transverse reinforcement were also tests. Two confinement details were tested: one using stirrups placed along entire splice length (a fully confined splice) and the other with stirrups placed at the ends of the lap zone (a locally confined splice). All of the specimens failed in a brittle and sudden manner. Failure occurred with a rapid loss of capacity. It was concluded that: The current design provisions do not give a conservative result for high-strength reinforcing bars, especially, without transverse reinforcement. While without transverse reinforcement, the head bearing cannot be activated due to *prying action*. By placing transverse reinforcement at ends of splice length, the end bearing contributions increased dramatically. For the fully confined splices where transverse reinforcement was placed along splice length, the end bearing contributions increased by 73% on average. Also, the bond strengths in unconfined splices were not developed completely due to prying action. However, if transverse reinforcement is provided, the bond strengths can be developed more than the bond strength of a straight bar.

Yassin (2013) [28] tested Eight simply supported reinforced concrete wide beams to study the behavior and strength of reinforced concrete wide beams with headed bar lap splice of tension reinforcement. The main studied variables were lap splices length, stirrups spacing in the lap splice zone, and cut off ratio. All beams were with dimensions 400 mm x 200 mm in cross section, and 2400 mm simply supported span. Figure (2-49) shows the longitudinal and cross-sectional details of some specimens. In studying the factor of lap splices length, length of lap splice was chosen as 8, 15.5, and 27 times the bar diameter, while for studying the effect of stirrups spacing in the lap splice zone, a spacing of 190 mm, 90 mm, and 45 mm were used. Moreover, the factor of cut off ratio, cut off percentages of 0.0% (No splice), 50%, and 100% were tested. From test results, it was concluded that:

1- The behavior of wide beam without splice can be achieved in spliced beam when: L_o = 27 d_b without using any stirrups and with 100 % cut off ratio, or L_o = 15.5 d_b using stirrups spacing (S) = 0.27 d and with 100 % cut off ratio, or L_o = 15.5 d_b without using any stirrups and with 50 % cut off ratio.
2- In spliced beams, the mode of failure changed from brittle (side blow out) failure to flexural failure when: L_o = 27 d_b without using any stirrups and with 100 % cut off

ratio, or L_o = 15.5 d_b using stirrups in the lap splice zone and with 100 % cut off ratio, or L_o = 15.5 d_b without using any stirrups and with 50 % cut off ratio.

3- Spliced beam showed increasing in the ultimate deflection and strain energy than un-spliced beam when: L_o = 27 d_b without using any stirrups and with 100 % cut off ratio, or L_o = 15.5 d_b using stirrups in the lap splice zone and with 100 % cut off ratio, or L_o = 15.5 d_b without using any stirrups and with 50 % cut off ratio.
4- Spliced beam showed a brittle (side blow out) failure and decreasing in the ultimate load and strain energy than un-spliced beam when: L_o = 15.5 d_b without using any stirrups and with 100 % cut off ratio, or L_o = 8 d_b without using any stirrups and with 100 % cut off ratio.

2.8.2 Application studies on headed bars

Haroun, et al. (2000) [15] tested six 1/2-scale cantilevered pier walls and loaded them in the weak direction under cyclic loading and taken to (near) destruction, as shown in Fig. (2-50). Five of the damaged pier walls were repaired with two alternating crossties at each crosstie location, whereas one of the damaged pier walls was repaired with T-headed reinforcing bars in place of regular crossties. The six repaired pier walls were retested under the same test protocol as the original samples to compare their performance. The six pier walls were divided into two groups. One group had a low vertical reinforcement ratio of 1.3%, while the other group had a high vertical reinforcement ratio of 2.3%. The 7'' (178 mm) spacing of the vertical reinforcing bars was the same for both groups, whereas No. 6 (19 mm) and 8 (25 mm) bars were used for the pier walls. Each pier wall sample was denoted with two letters: the first letter of L or H indicated either the low or high vertical reinforcement ratio, whereas the second letter, N (none), P (partial), or U (uniform), indicated the cross tie distributions. A 25 in. height of concrete, a few inches more than the calculated plastic hinge length, was removed from the base of the shored pier wall. The crossties were placed such that it hooked around the horizontal bars, show Fig. (2-51). The T-headed reinforcement consisted of two square steel plates friction-welded to either end of a section of standard reinforcing steel. The head of the T-headed crosstie used was 2 x 2 x 0.5 in. The ratio A_h/A_b = 13 is based upon a head area A_h of 4.0 in^2, and a bar area A_b of 0.31 in^2, as shown in Fig. (2-52). From test results, it was concluded that:

1- The strength and displacement of the repaired L walls were similar to the original L walls. The strength of the repaired H walls was higher than the strength of the original H walls; the displacement of the repaired H walls was lower than the displacement of the original H walls.
2- Pier walls with average to low vertical reinforcement ratios can be repaired with little or no loss of lateral load capacity or displacement ductility.
3- T-headed crosstie reinforcement performed as well or better than, the regular crosstie reinforcement.

Chun, et al. (2004) [5] tested four large- scale exterior beam-column joints. To evaluate the performance of the mechanical anchor compared with that of the conventional standard hook. The new mechanical anchor is shown in Fig. (2-53), with the minimum head plate, was proposed. The specimens represent sub-assemblies of a building subjected to lateral loads. Two sets of exterior beam-column joints were tested. One set (JC-1, JM-1) was designed so

that flexural failure of beam would occur, while the other set (JC-2, JM-2) was designed so that shear failure of joint would occur. The specimens of each set have the same geometry and the same material properties. The structural performance, such as strength, stiffness, ductility, slip of re-bars, the extent of joint damage and the energy dissipation were assessed. The 90-degree standard hook was designed according to ACI, and the development length of mechanical anchor was three quarters of the column depth. The overall dimensions for the specimens and the reinforcement details are showed in Fig. (2-54).The cyclic lateral loads were applied to the beam. It was concluded that: From this study, it was validated that the mechanical anchor, in place of the standard hook, has enough anchorage capacity within the exterior beam-column joints. Especially, the mechanical anchor has better capacity than the standard hook of which the extension is placed outward from the joint.

Seo, et al. (2004) [19] tested eight deep beam specimens with headed reinforcements for mechanical anchorage and two general deep beam specimens with standard hook. The beams were designed to investigate whether the standard hook anchorage designed according to ACI 318-02 at the ends of the positive moment region can be replaced with mechanical anchorage using steel head and to estimate the shear behavior of deep beams. The experimental variables were: anchorage type of longitudinal reinforcement, shear span-to-overall height (a/h), vertical shear reinforcement ratios ρ_v and horizontal shear reinforcement ratios ρ_h. All specimens had rectangular cross section with size of 160 mm × 600 mm × 2500 mm as shown in Fig. (2-55). Specimens were classified into two groups according to the anchorage type of longitudinal reinforcement. The first one group (A) was the group designed to have longitudinal reinforcement with 90-degree hooks and the second group (M) was with mechanical anchorage. In the specimen details, vertical shear reinforcement was designed as closed stirrups type of 10 mm deformed bars, while the horizontal shear reinforcement is straight type of 10 mm deformed bars. From test results, it was concluded that on comparing the case with 90-degree hook anchorage, the specimen with headed reinforcement as a mechanical anchorage showed better load resistance capacity when it was designed to satisfy the development length requirement of the ACI code.

Li, et al. (2010)[18] tested eight reinforced concrete beam specimens connected with either lapped headed reinforcement or lapped welded wire reinforcement tested along with a specimen reinforced by continuous bars for comparison. They focused on improving continuous longitudinal joint details for decked precast prestressed concrete girder bridge systems. For a typical DBT (Decked Bulb Tees), the compressive strength of the deck flange and the grout is 49 MPa. d_b = 16 mm-diameter epoxy coated bar with yielding stress 420 MPa were lapped in the 152 mm deep flange joint, the development length L_d for straight bar and hooked bar are 546 mm and 273 mm , respectively. Figure (2-56-a) shows the U bars spliced with the transverse deck reinforcement in the top flange of the DBT. They were bent to contact with the opposite U bars in the adjacent girder. Two longitudinal bars were laced through the interlocking U bars. Figure (2-56-b) shows a non-overlapping headed bar connection detail proposed for consideration. Two layers of transverse deck reinforcement were projected out of the top flange of the girder with a head on the end. The adjacent girders was placed with the opposing headed bar abutting each other. One welded wire reinforcement (WWR) is spliced with each layer of headed bar for force transfer. Figure (2-56-c) shows a proposed joint detail with spirals confining lapped splices. Figure (2-57) shows a model specimen in two adjacent DBTs with the dashed line representing the longitudinal joint. Figure (2-58) shows details of the three types of specimens. For the headed bar detail, the

primary variables were the lap length and the spacing of the reinforcement. The headed reinforcement was 16 mm-diameter bar with a standard 51 mm-diameter circular friction welded head. The head thickness was 13 mm. For the WWR the lap length was reduced to 102 mm. The spacing of WWR was the only variable in the second type of specimen. The diameter of WWR reinforcement is 16 mm. A control specimen with a layer of continuous 16 mm diameter rebar with a spacing of 152 mm across the joint zone shown in Fig. (2-58-c) was tested for comparison purpose. All specimens were simply supported with a 2.438 mm span as shown in Fig. (2-59) .Two kinds of failure occurred Fig. (2-60) showed display the ductile, slow failure and the sudden, brittle failure, respectively. From test results, it was concluded that:

1- The headed bar detail can provide a continuous force transfer in the longitudinal joint for DBT bridge system while minimizing the width of the joint to accelerate DBT bridge construction.
2- The lap length for the headed bar detail is recommended to be 152 mm . This lap length provided full development of the bars to produce full load capacity and significant ductility.
3- The reinforcement spacing had an effect on the structural behavior. The smaller spacing provided more load resistance with less ductility because more steel was provided in the same cross section.

Table 2-1: Lap splice requirements as recommended by different building Codes

	Egyptian Code 203-2007	**ACI 318-2014**	**Eurocode 2-2004**	**CSA A23.3-04**
Development length(L_d)	$L_d = \frac{\alpha.\beta.\eta.f_y/1.15}{4.f_{bu}}\ d_b$	$L_d = (\frac{fy}{1.1\lambda\sqrt{f_c'}} * \frac{\Psi_t \Psi_e \Psi_s}{(\frac{c_b+K_{tr}}{d_b})})d_b$	$L_d = \frac{d_b}{4} * \frac{f_s}{f_{bd}}$	$L_d = 1.15\frac{k_1 k_2\ k_3\ k_4}{(d_{cs}+k_{tr})}\frac{f_y}{\sqrt{f_c'}}A_b$
Development length of headed bars (L_{dt})	Not included	$L_{dt} = \frac{0.19\Psi_e f_y}{\sqrt{f_c'}}\ d_b$	No include this type of bars	include this type of bars but without equation
Lap splice length(L_o)	L_o=L_d If $A_{s\ provided} \geq 2\ A_{s\ required}$ L_o=1.3L_d If $A_{s\ provided} < 2\ A_{s\ required}$	Class A: L_o=1.0 L_d Class B: L_o=1.3 L_d	$L_o = \alpha_1\alpha_2\alpha_3\alpha_5\alpha_6\ L_d \frac{A_{s\,req}}{A_{s\,prov}}$	Class A: L_o=1.0 L_d Class B: L_o=1.3 L_d
Staggered distance	≥ 1.3 L_o	≤ 600 mm	≥ 1.3 L_o	≤ 600 mm
Clear distance between bars in one lap	≤ 150 mm ≤ 0.2 L_o	≤ 150 mm ≤ 0.2 L_o	≤ 50 mm ≤ 4 d_b	≤ 150 mm ≤ 0.2 L_o
Clear distance between two adjacent laps	----------	----------	In case of adjacent laps ≥ 2 d_b ≥ 20 mm	----------
Cut off ratio along the lap length	Allow 100%, and no restriction in Number of layers	≤ 100%	Allow up to 100% if the bars are all in one layer. Where the bars in several layers the percentage should be reduced to 50%	≤ 100%
Cut off ratio in one section	≤ 25% for L_o=L_d > 0.25% for L_o≥ 1.3 L_d	≤ 50% if Class A ≤ 100% if Class B	≤ 50%	≤ 50% if Class A ≤ 100% if Class B
Notes	• If d_b≥ 28 mm lap splices are not allowed. • Lap splices in sections subjected to direct tension are not allowed.	• If d_b ≥ 36 mm lap splices are not allowed.		• If d_b ≥ 35 mm lap splices are not allowed.

Table 2-2: Definition of Class A and Class B, according to ACI 318-14[2]

$A_{s\ provided}$ / $A_{s\ required}$*	Maximum percentage of A_s spliced within the required lap length	
	50	100
Equal to or greater than 2	Class A	Class B
Less than 2	Class B	Class B
*Ratio of area of reinforcement provided to area of reinforcement required by analysis at splice location		

Table 2-3: The required development length and required lap splice length

Building Codes	Calculated development length	Calculated lap splice length
Egyptian Code 203-2007	$L_d = \frac{\alpha.\beta.\eta.f_y/1.15}{4.f_{bu}} d_b$ $= \frac{1.0*0.75*1.0*(\frac{400}{1.15})}{4*1.34} * 10 = 490$ mm	$L_o = 1.3L_d$ $L_o = 637$ mm
ACI 318-2014	$L_d = (\frac{fy}{1.1\lambda\sqrt{f_c'}} * \frac{\Psi_t \Psi_e \Psi_s}{(\frac{C_b + K_{tr}}{d_b})})d_b$ $=(\frac{400}{1.1*1.0*\sqrt{24}} * \frac{1.0*1.0*0.80}{2.50}) * 10$ $= 237$ mm <300 mm Used $L_d = 300$ mm	Cut off 100% used Class B $L_o = 1.3L_d$ $L_o = 390$mm
Eurocode 2-2004	$L_d = \frac{d_b}{4} * \frac{f_s}{f_{bd}}$ $= \frac{10}{4} * \frac{400/1.15}{2.7} = 320$ mm	$L_o = \alpha_1\alpha_2\alpha_3\alpha_5\alpha_6 L_d \geq (L_{o\ min=200mm})$ $= 1.0*0.78*1.0*1.0*1.5*320$ $= 374$ mm
CSA A23.3-04	$L_d = 1.15 \frac{k1\,k2\,k3\,k4}{(d_{cs}+k_{tr})} * \frac{f_y}{\sqrt{f_c'}} A_b =$ $(1.15*1.0*1.0*1.0*0.8/25)$ $*(400/4.9)*10 = 236$ mm < 300 mm Used $L_d = 300$ mm	Cut off 100% used Class B $L_o = 1.3L_d$ $L_o = 390$ mm
Note: development length of headed bars in ACI 318-14; $L_{dt} = \frac{0.19\Psi_e f_y}{\sqrt{f_c'}} d_b = \frac{0.19*1.0*400}{\sqrt{24}} * 10 = 155$ mm.		

The above values are for:
- $f_{cu} = 30$ MPa.
- $f_c' = 24$ MPa.
- $f_y = 400$ MPa.
- deformed bars.
- $d_b = 10$ mm

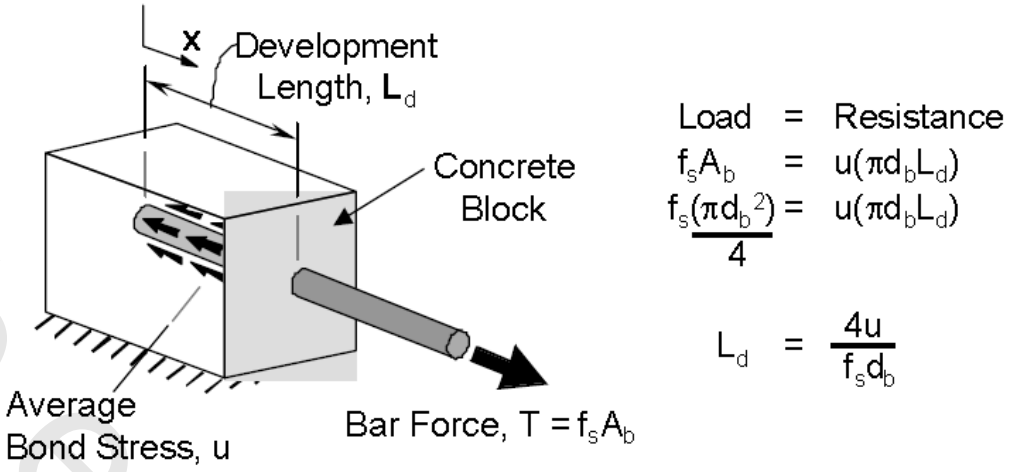

Figure (2-1): simply concept of bond stresses, after Thompson (2002) [22]

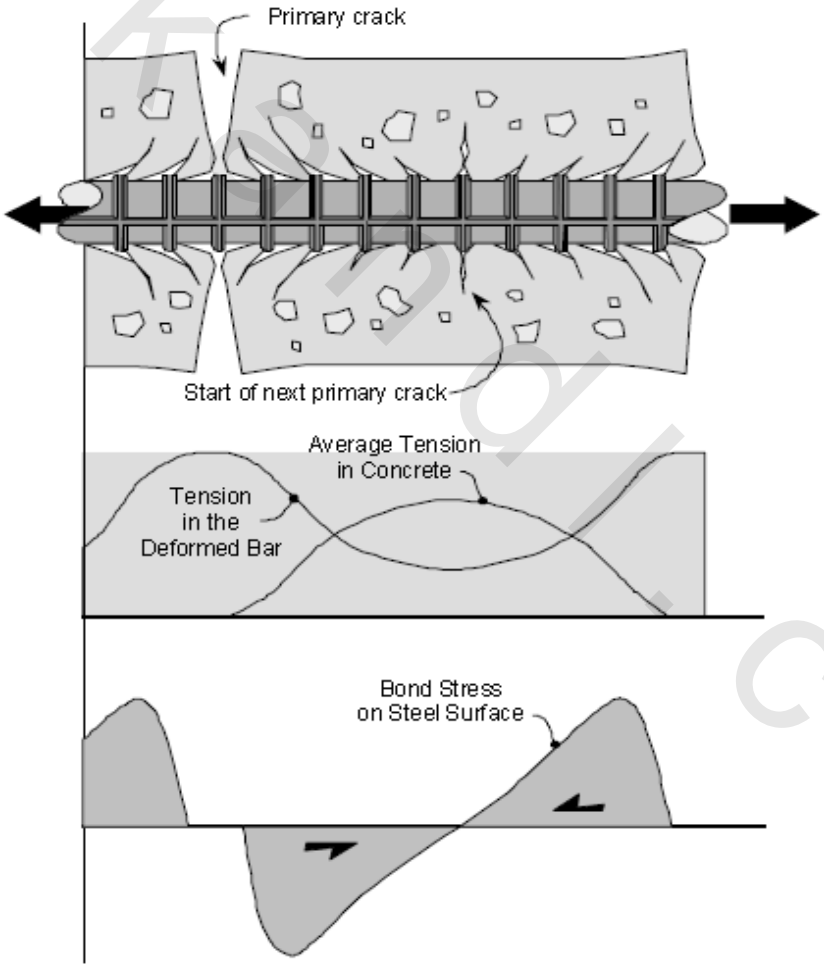

Figure (2-2): Transverse cracking at deformation, after Goto (1971) [12]

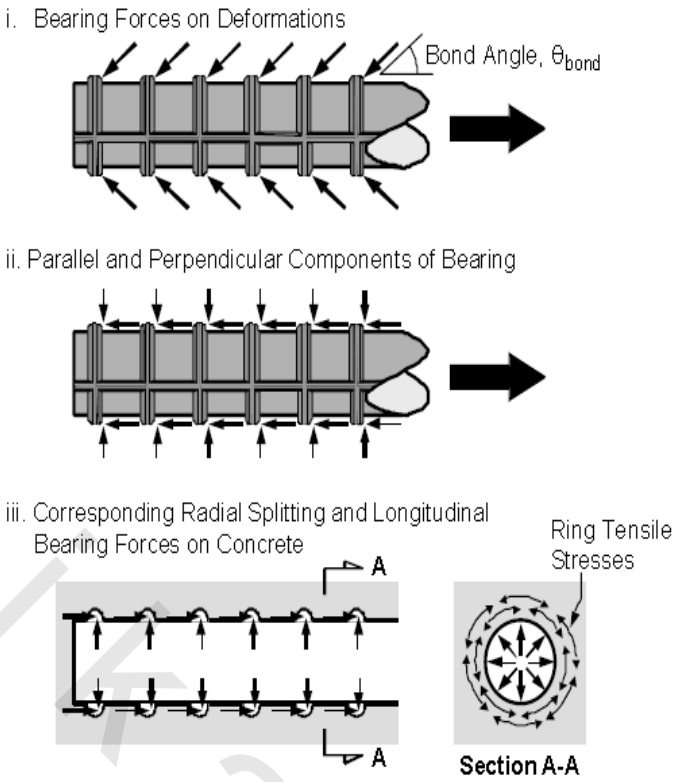

Figure (2-3): Bond and splitting components of rib bearing stresses, after Thompson (2002) [22]

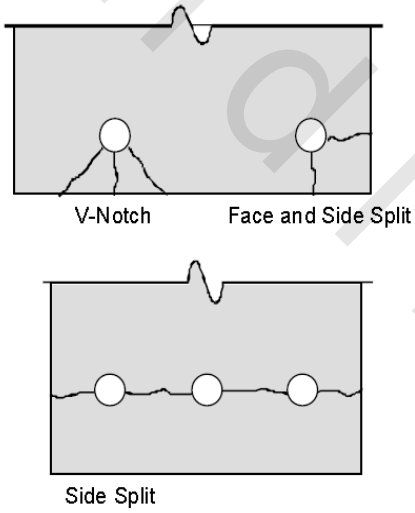

Figure (2-4): Possible splitting crack failures, after Thompson (2002) [22]

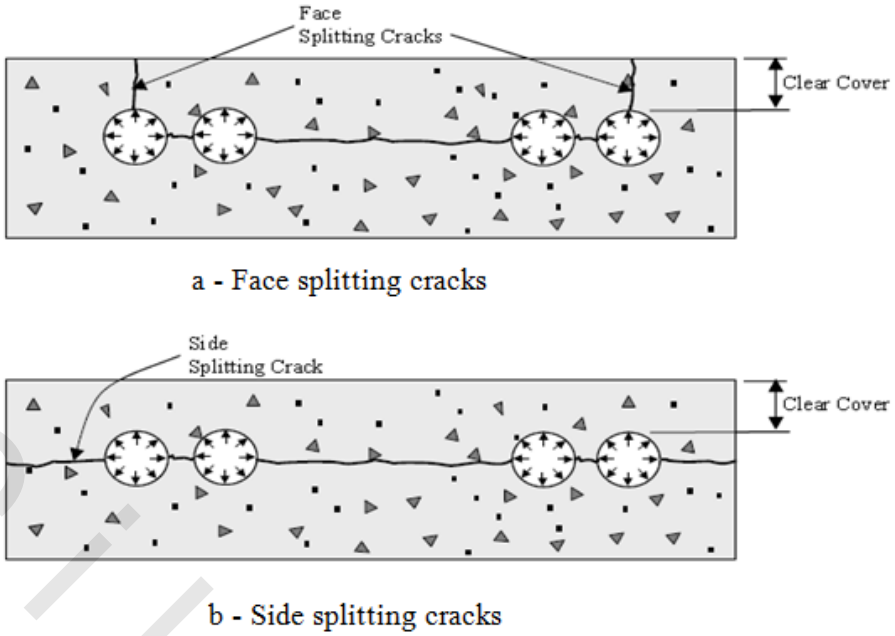

Figure (2-5): Splitting Cracks Caused by Radial Forces Acting on Concrete, by ledesma(2000)[17]

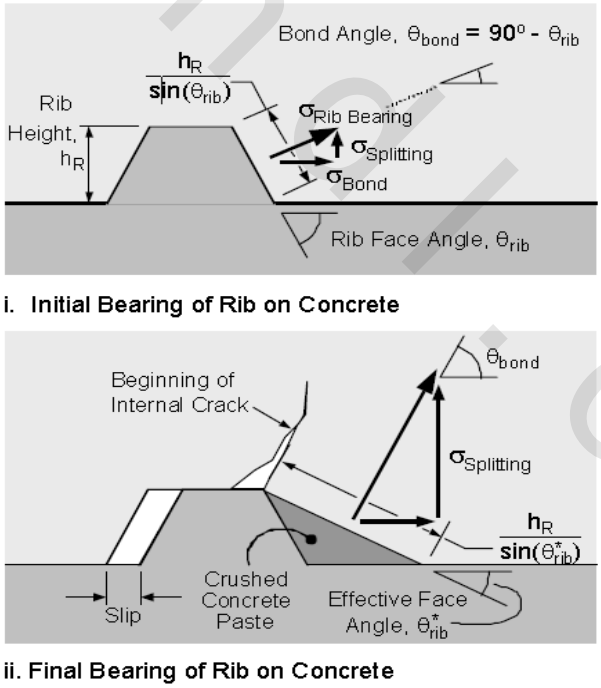

Figure (2-6): Mechanics of rib bearing on concrete, after Thompson (2002) [22]

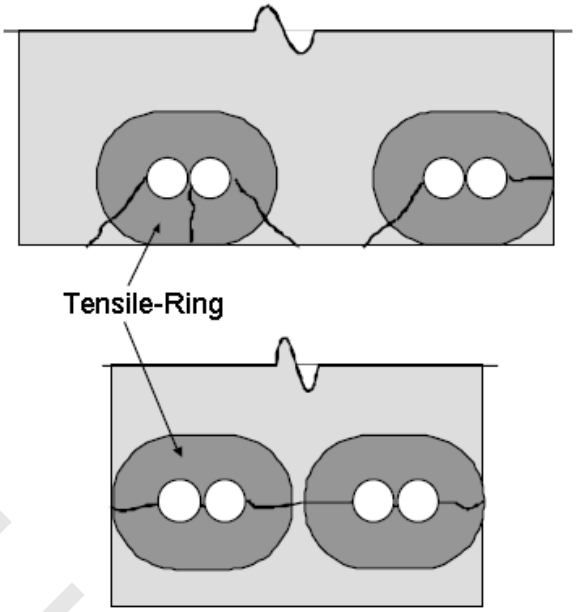

Figure (2-7): Splitting around lapped bars,after thompson (2002)[22]

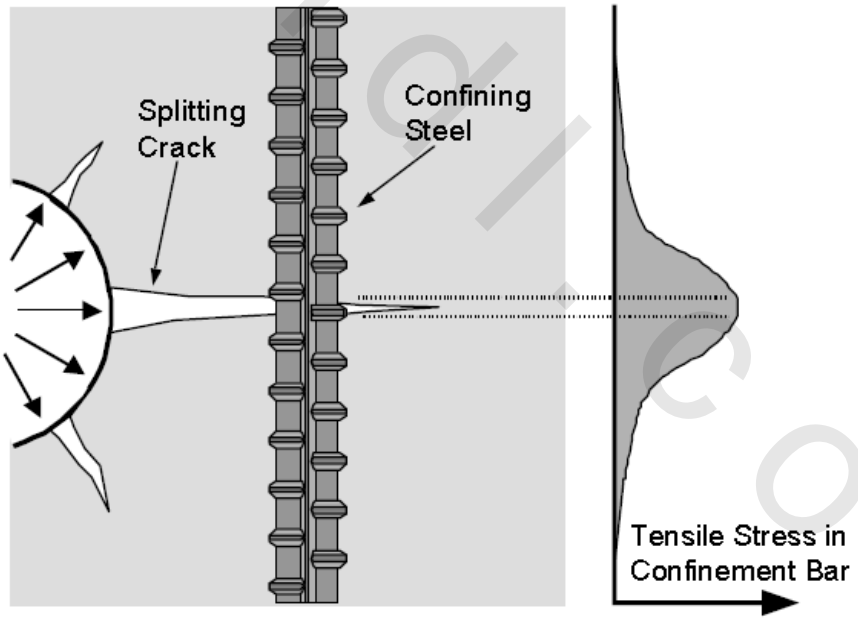

Figure (2-8): Confinement steel in the vicinity of a splitting crack, after Thompson (2002) [22]

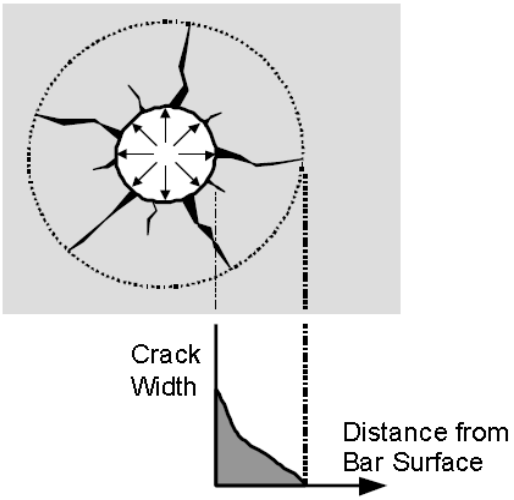

Figure (2-9): **Crack widths of splitting cracks, after Thompson(2002)[22]**

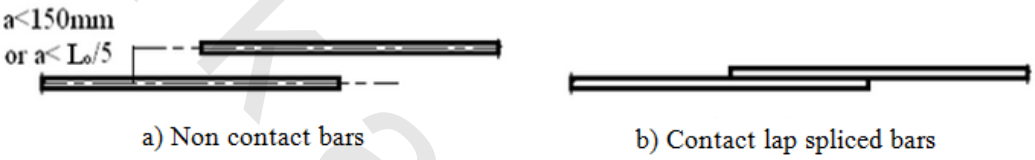

Figure (2-10): **The maximum clear distance between lapped bars in Egyptian Code, ECP 203-2007[9]**

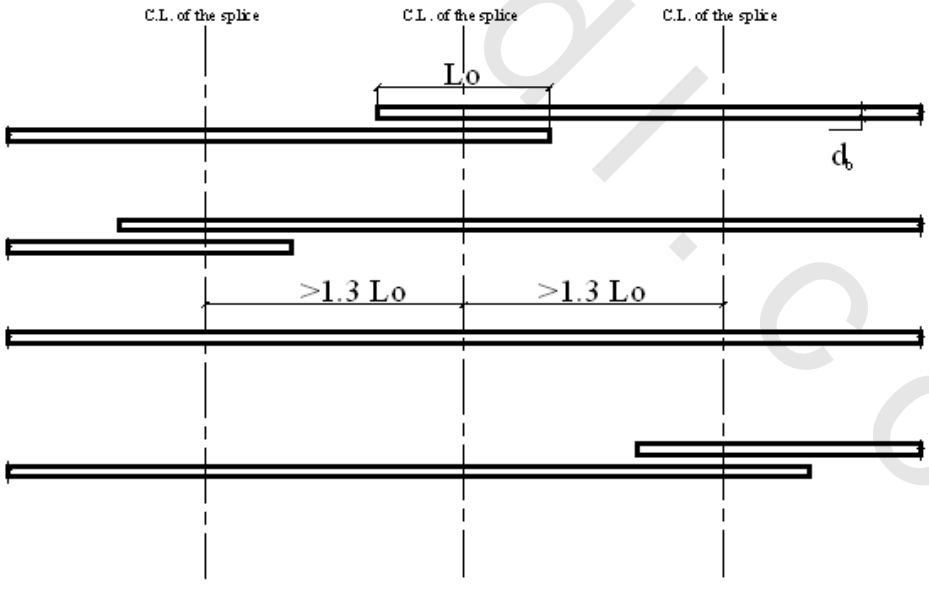

Figure (2-11): **The recommended arrangement of lapped reinforcement in Egyptian Code, ECP 203-2007[9]**

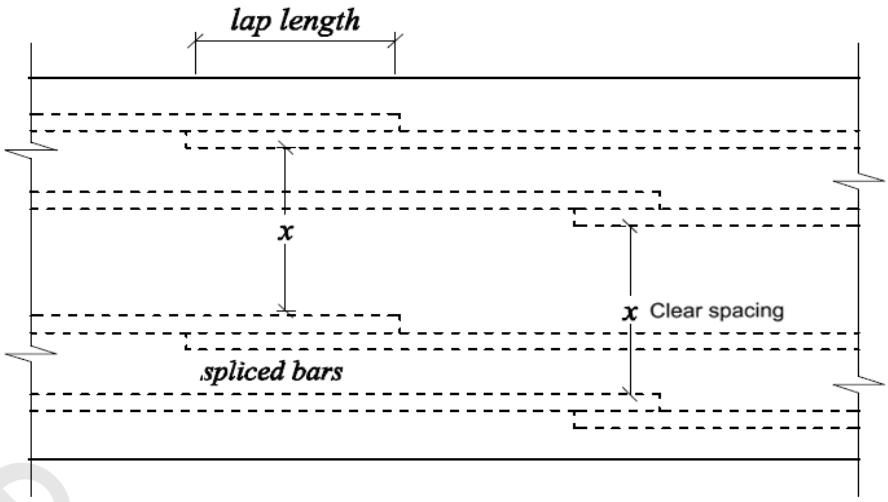

Plan

Figure (2-12): The recommended arrangement of lapped reinforcement in ACI 318-14[2]

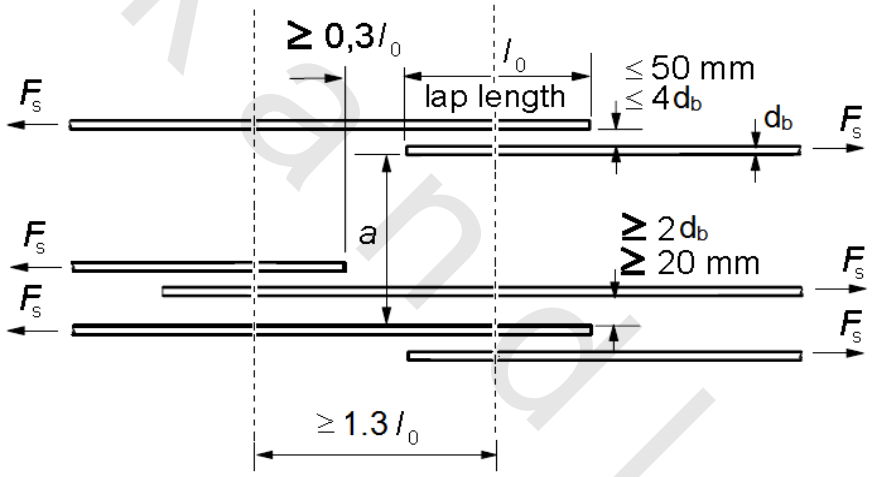

Figure (2-13): The recommended arrangement of lapped reinforcement according to Eurocode 2- 2004[10]

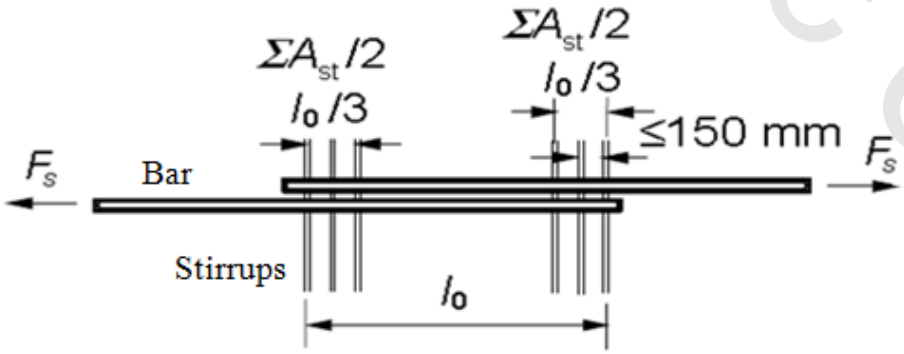

Figure (2-14): Transverse reinforcement for lapped splices according to Eurocode 2-2004[10]

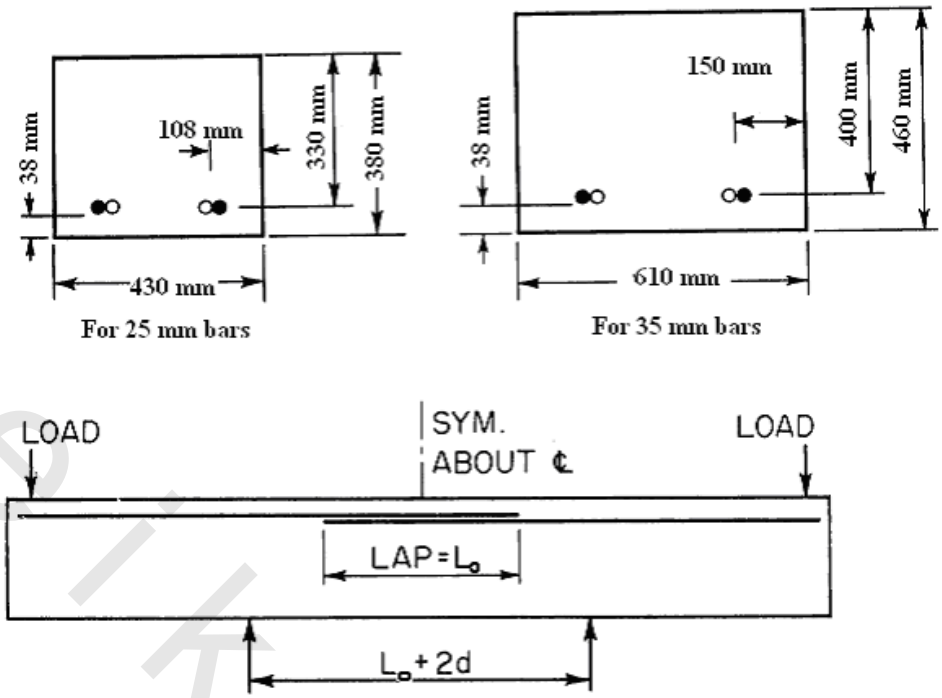

Figure (2-15): Beams tested by Ferguson et al (1965) [11]

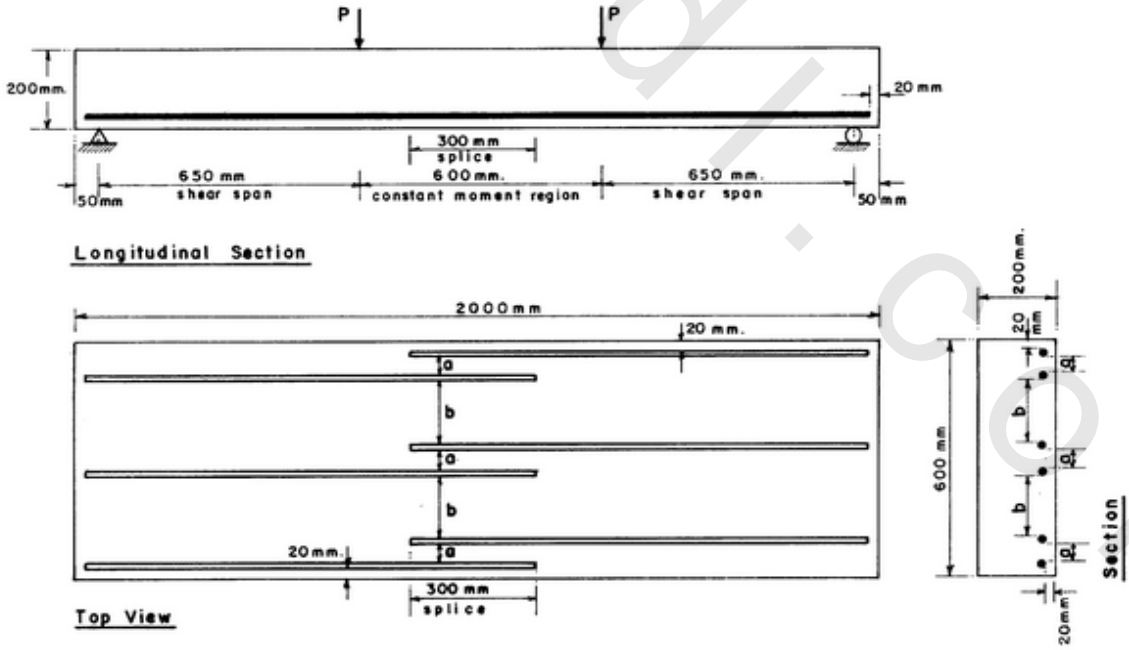

Figure (2-16): Details of specimens conducted by Hamad et al (1996) [14]

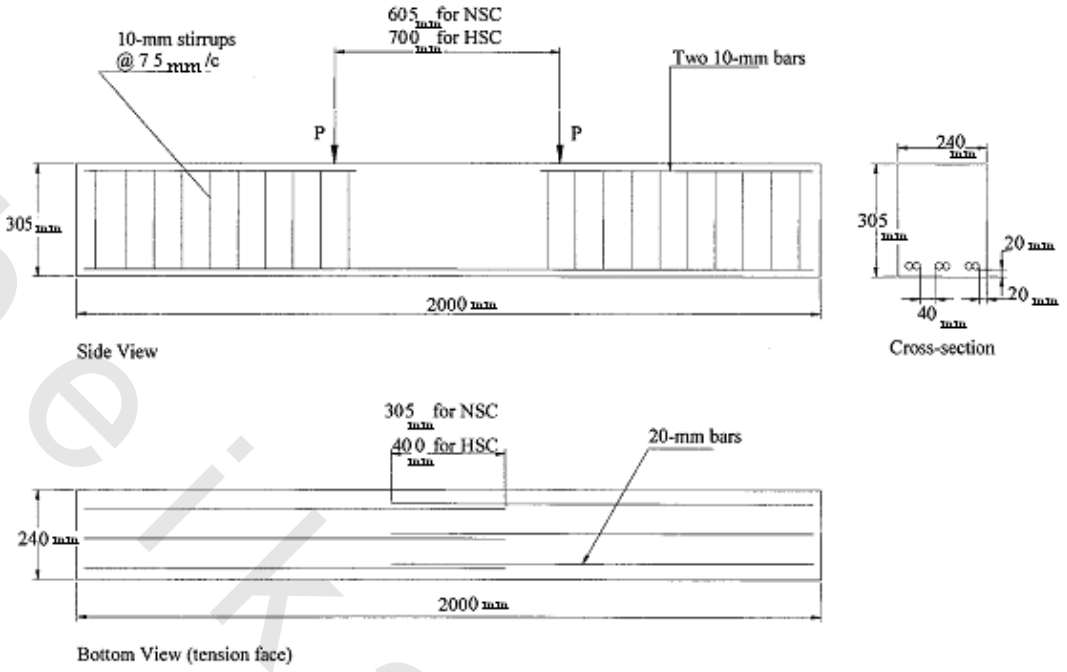

Figure (2-17): Details of beams tested by Hamad et al (2003) [13]

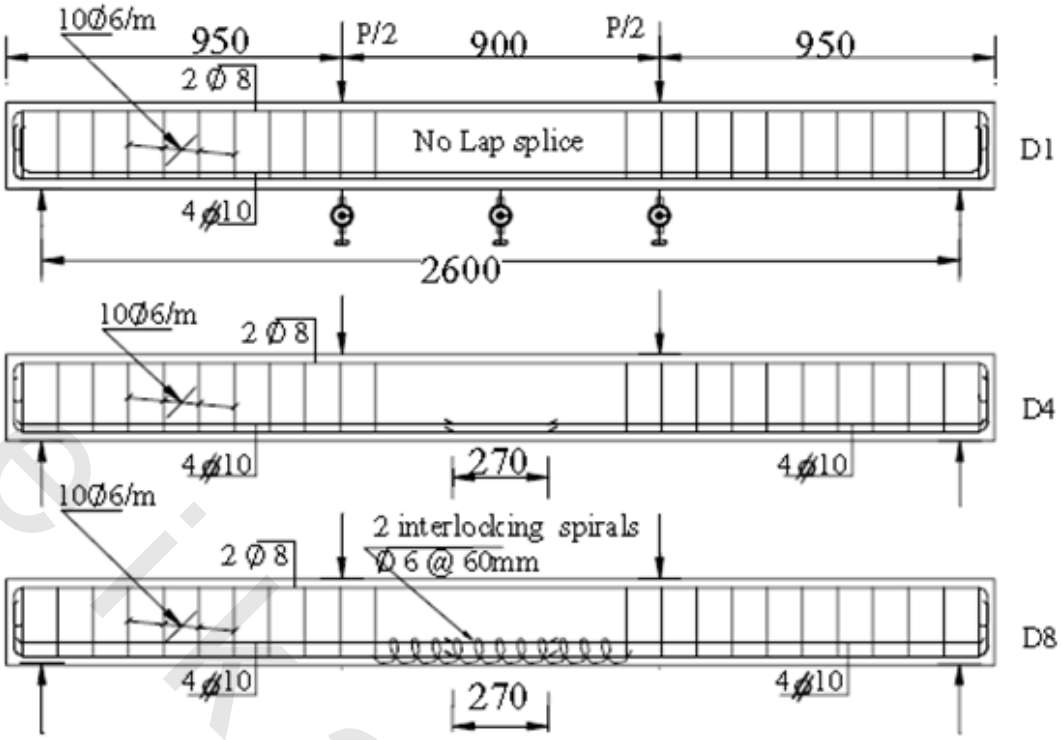

a- Details of some tested specimens

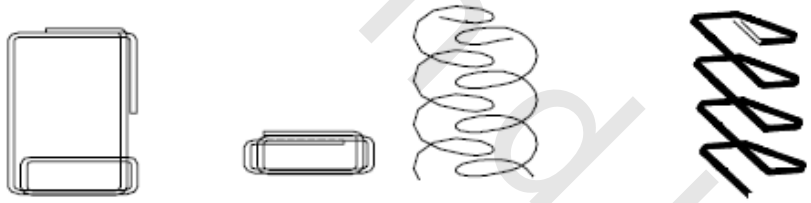

i. Stirrup shape

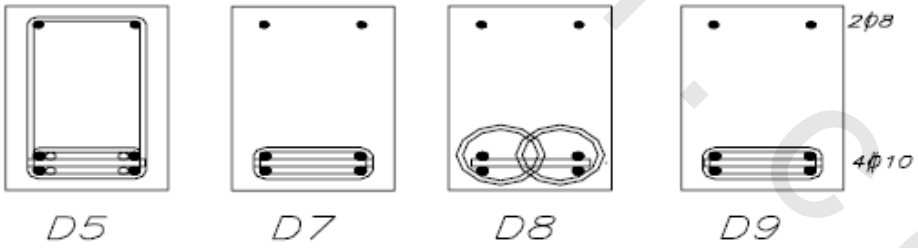

ii. Sections

b- Details of transverse reinforcement

Figure (2-18): Details of beams tested by Tarabia et al (2010) [21]

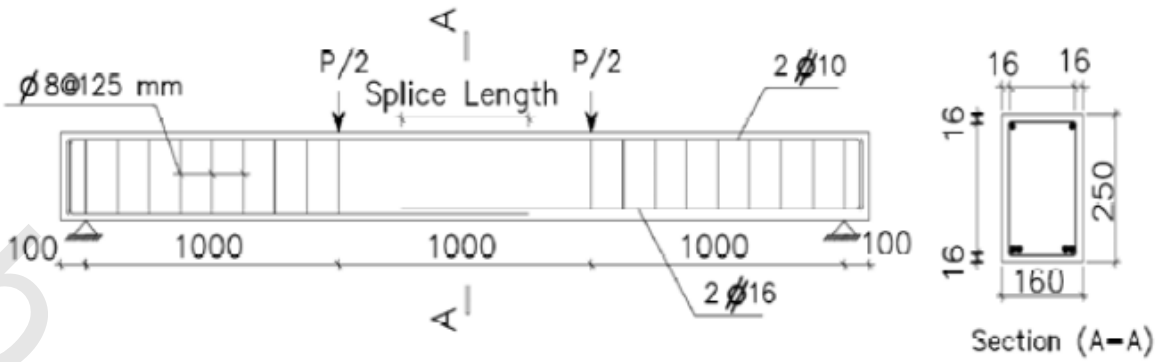

Figure (2-19): Longitudinal and cross section details of beam specimens tested by Abdel-Kareem et al (2013) [1]

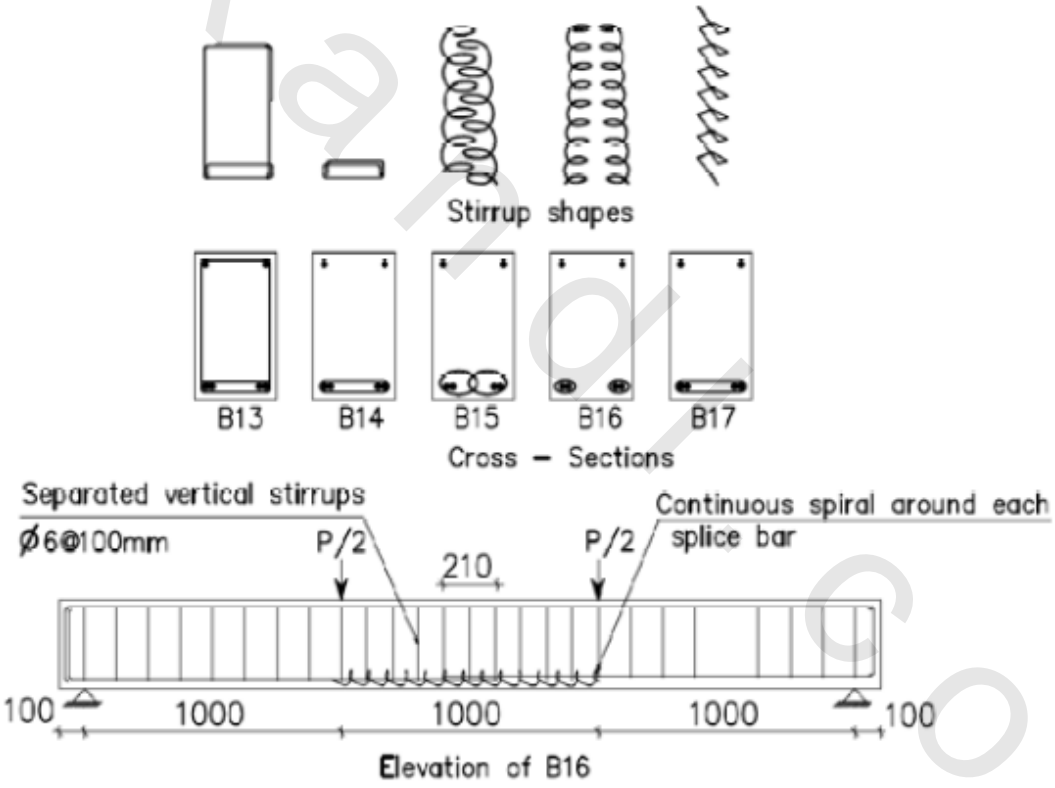

Figure (2-20): Details of stirrups around spliced bars used by Abdel-Kareem, et al (2013) [1]

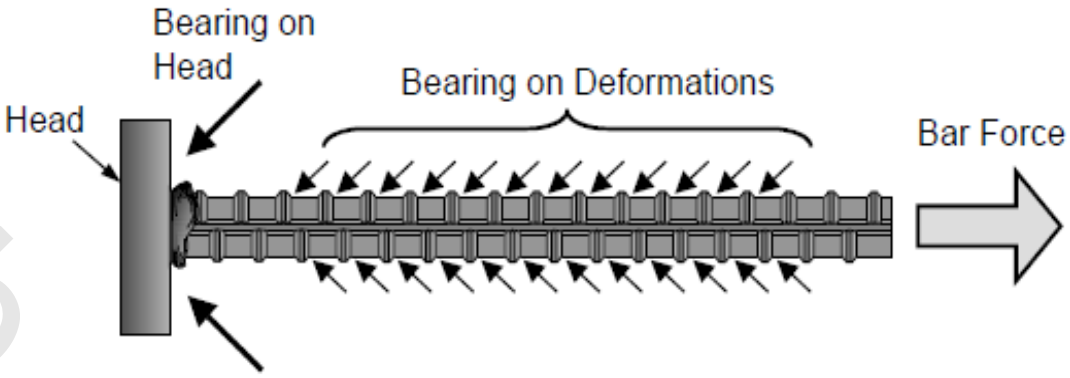

Figure (2-21): Anchorage of a headed bar by Thompson (2002) [22]

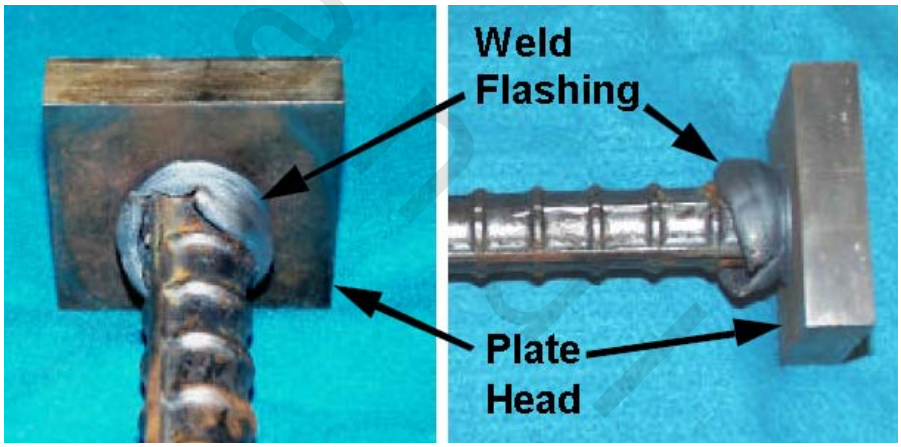

Figure (2-22): Friction-welded heads by Thompson et al (2002) [24]

Figure (2-23): Forged Head by Ledesma (2000) [17]

Figure (2-24): Threaded Head by Thompson et al (2002) [24]

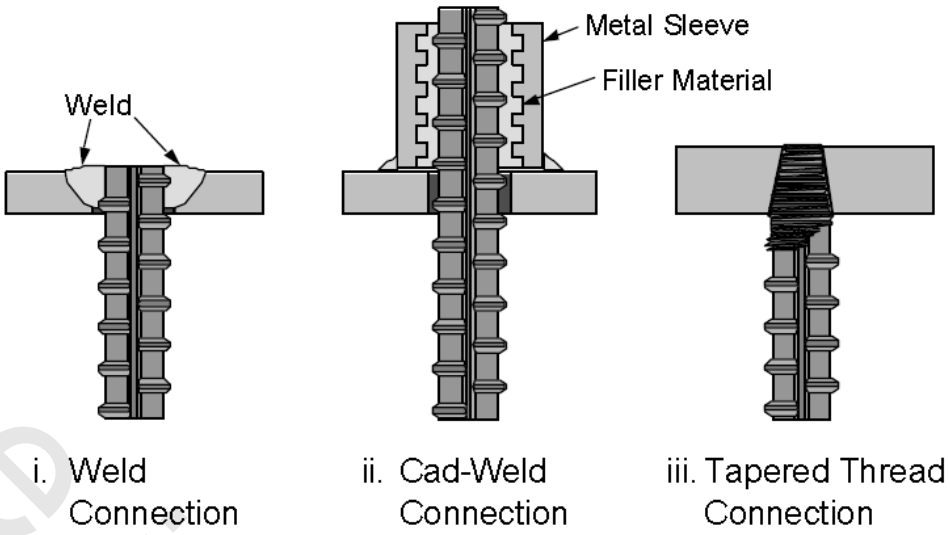

Figure (2-25): Head-bar connections tested by Caltrans [20]

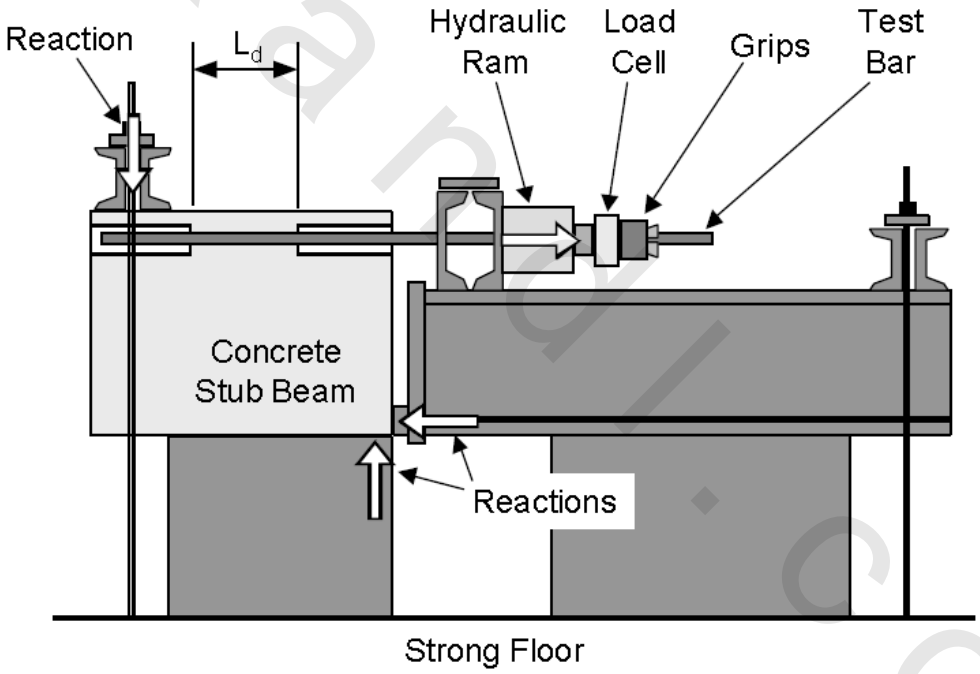

Figure (2-26): Typical beam-end test by Caltrans [20]

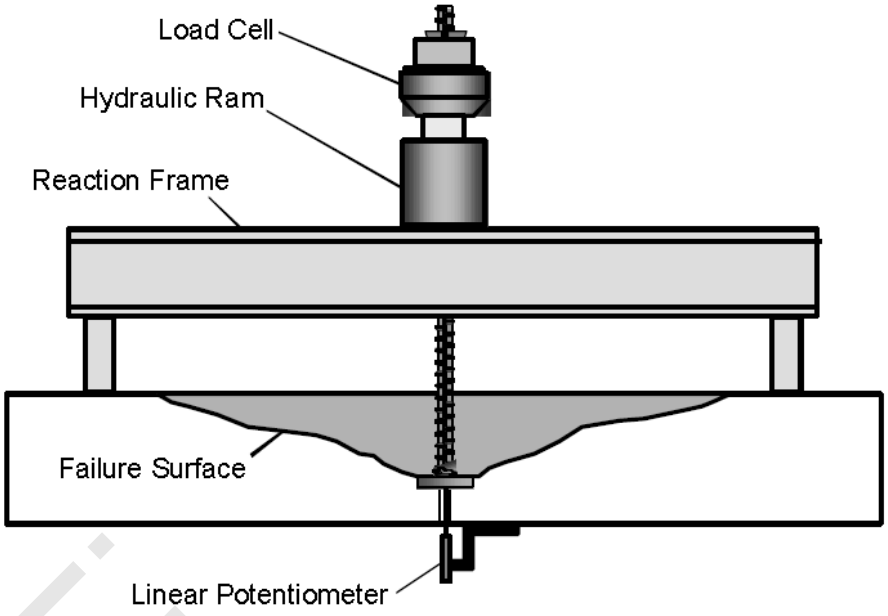

Figure (2-27): Shallow embedment pullout specimen used by Devries (1996) [8]

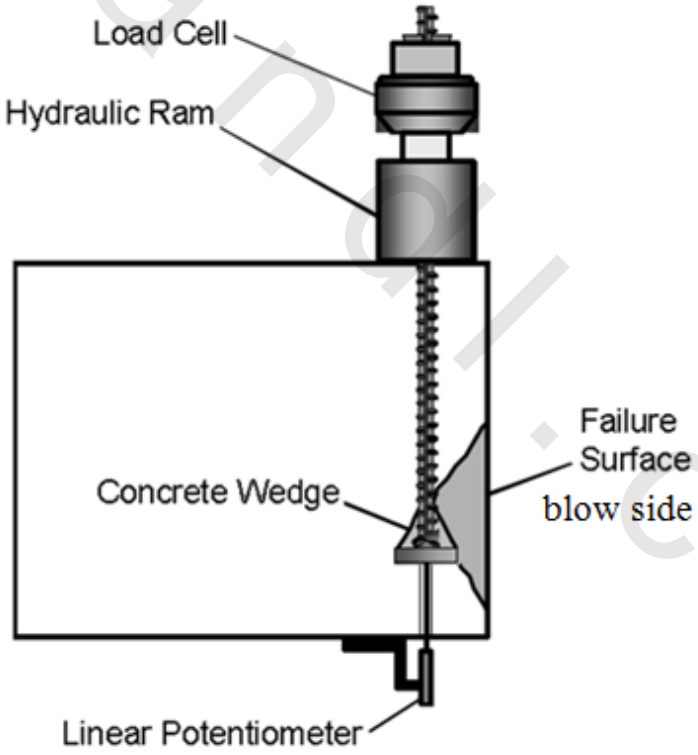

Figure (2-28): Deep embedment pullout specimen used by Devries (1996) [8]

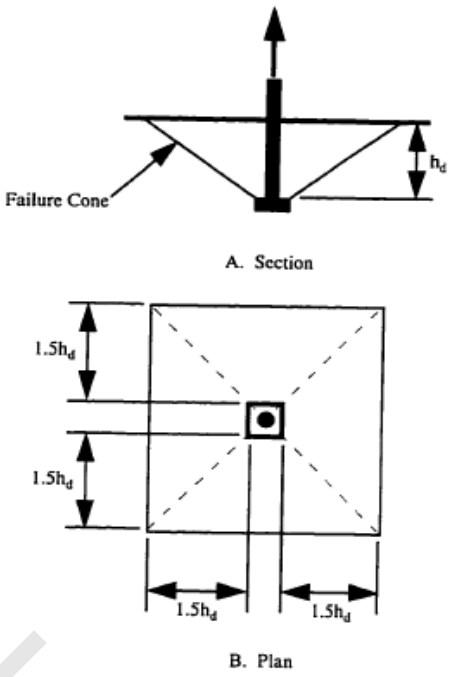

Figure (2-29): Pullout-cone failure for headed reinforcement used by Devries (1996) [8]

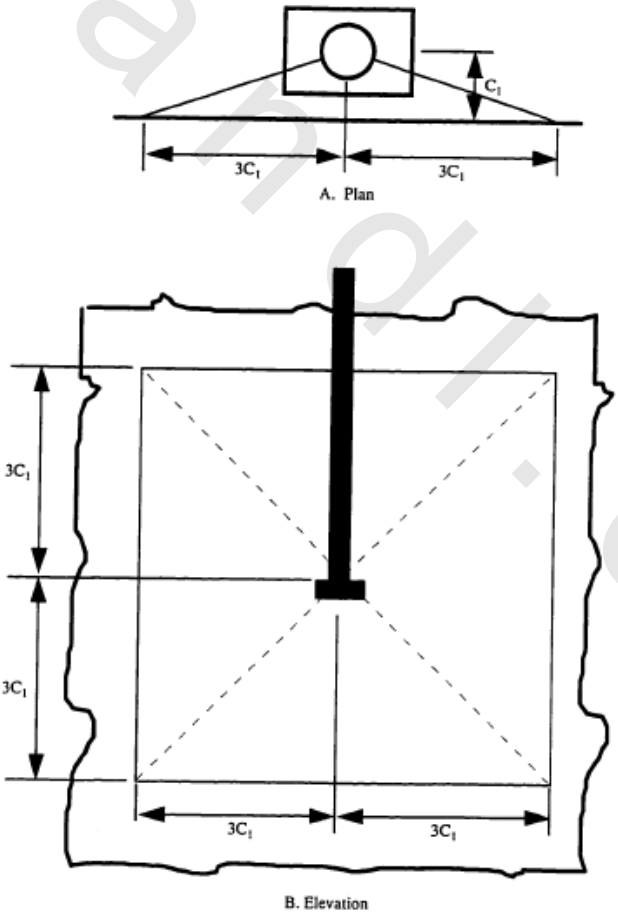

Figure (2-30): Blowout failure for headed reinforcement used by Devries (1996) [8]

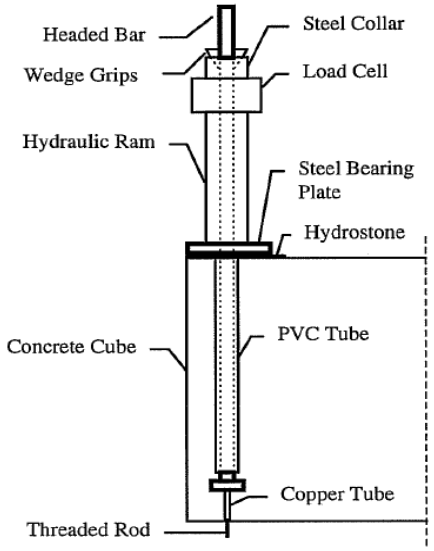

Figure (2-31): Test setup for pullout tests by Bashandy (1996) [3]

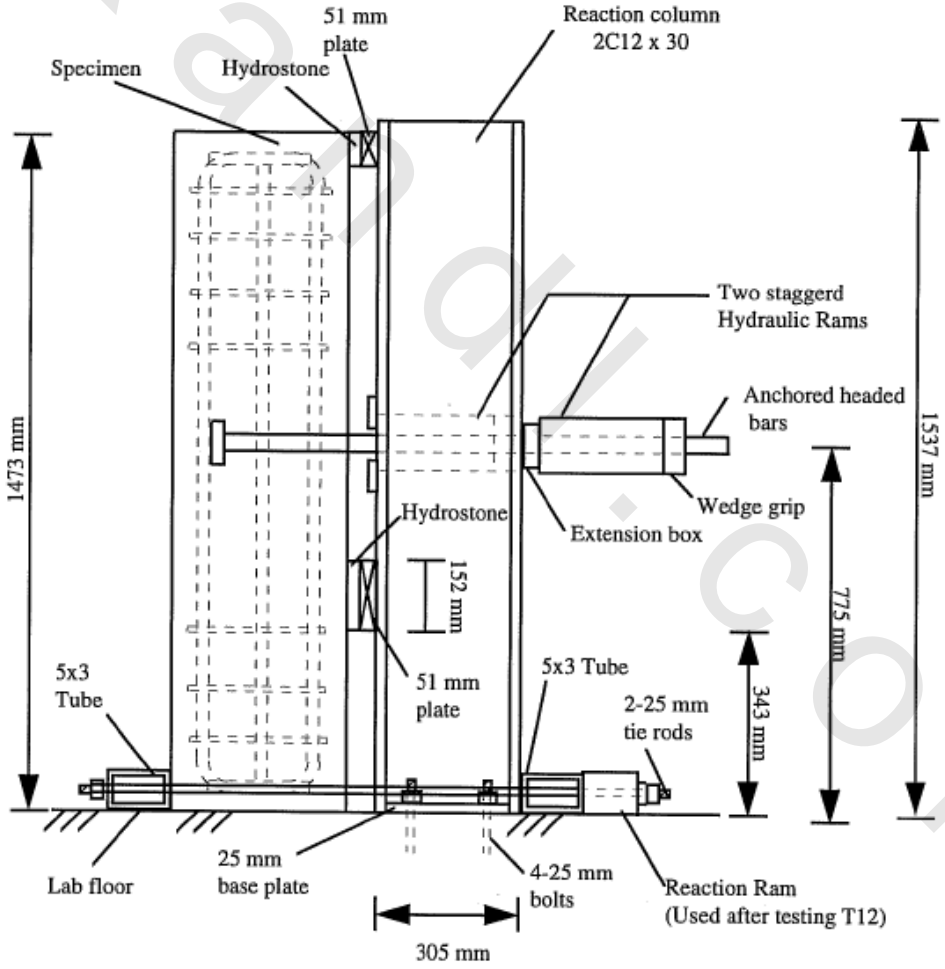

Figure (2-32): Test setup for the simulation exterior joints by Bashandy (1996) [3]

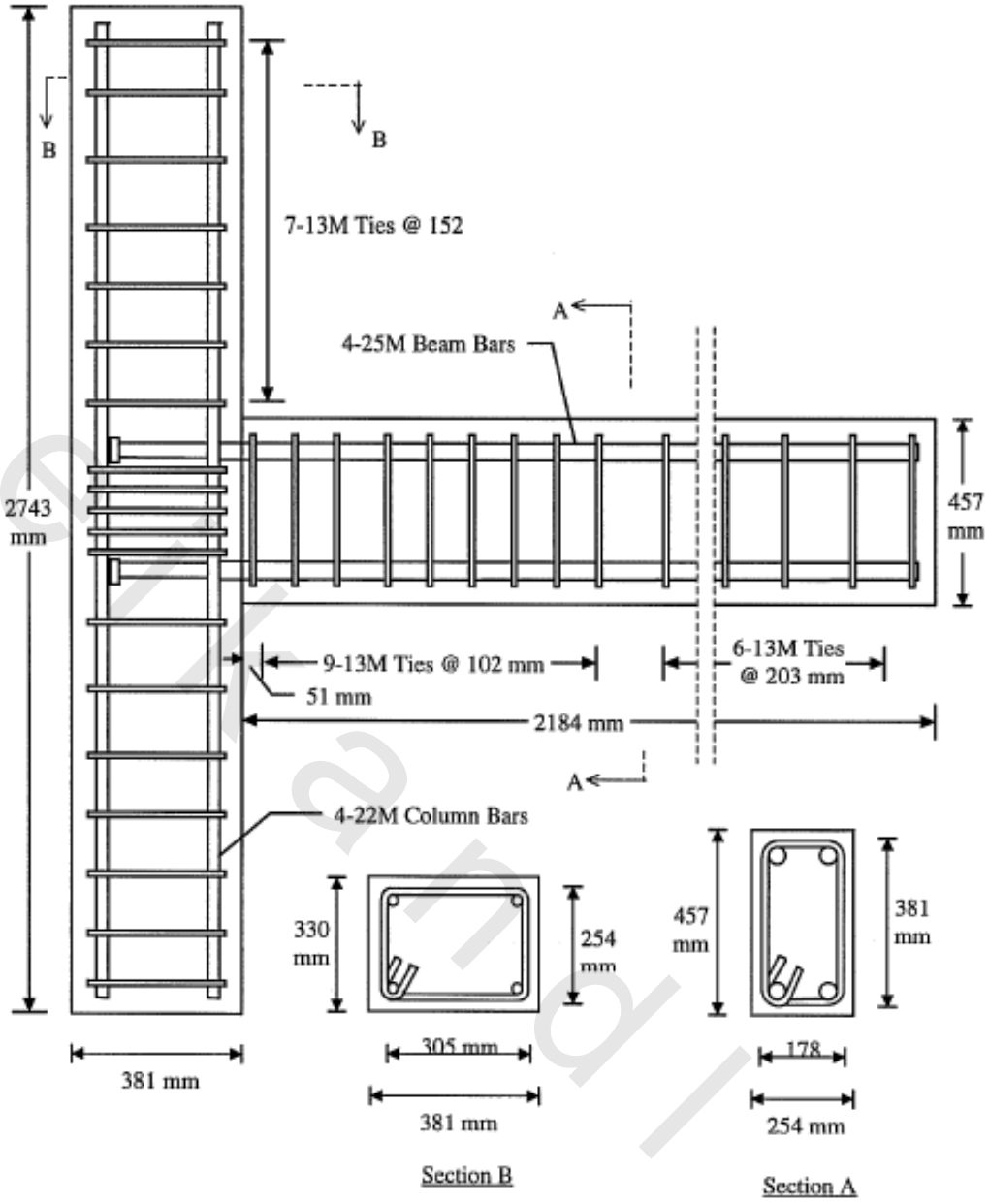

Figure (2-33): Concrete dimensions and reinforcement details of the headed bar specimen tested by Bashandy (1996) [3]

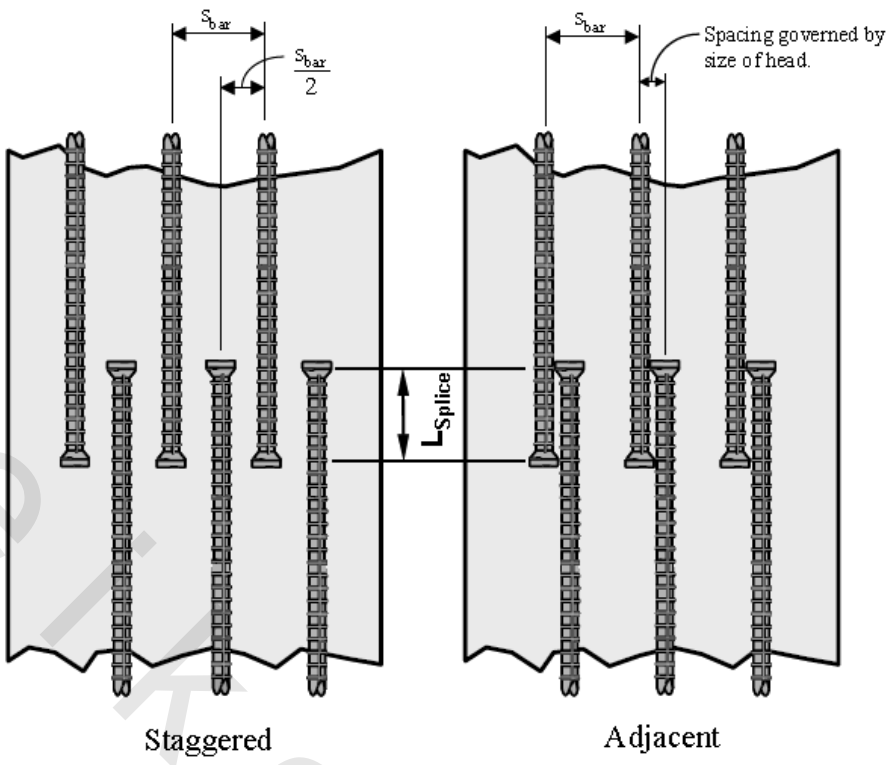

Figure (2-34): Staggered vs. Adjacent Spacing of Lap Splice by Ledesma (2000) [17]

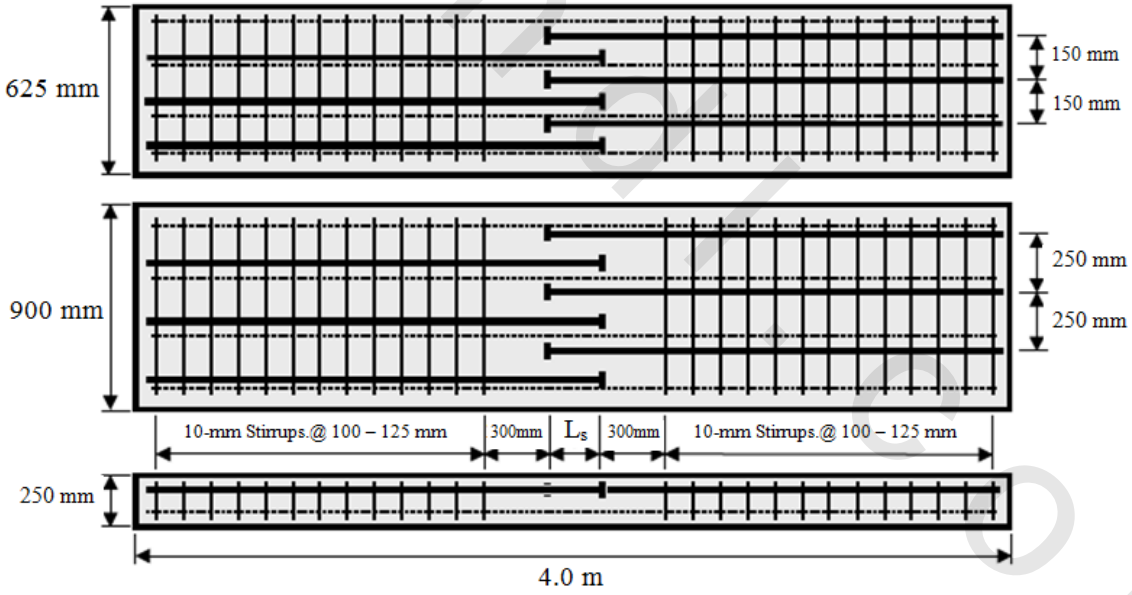

Figure (2-35): Reinforcement layout for staggered lap splices specimens by Ledesma (2000) [17]

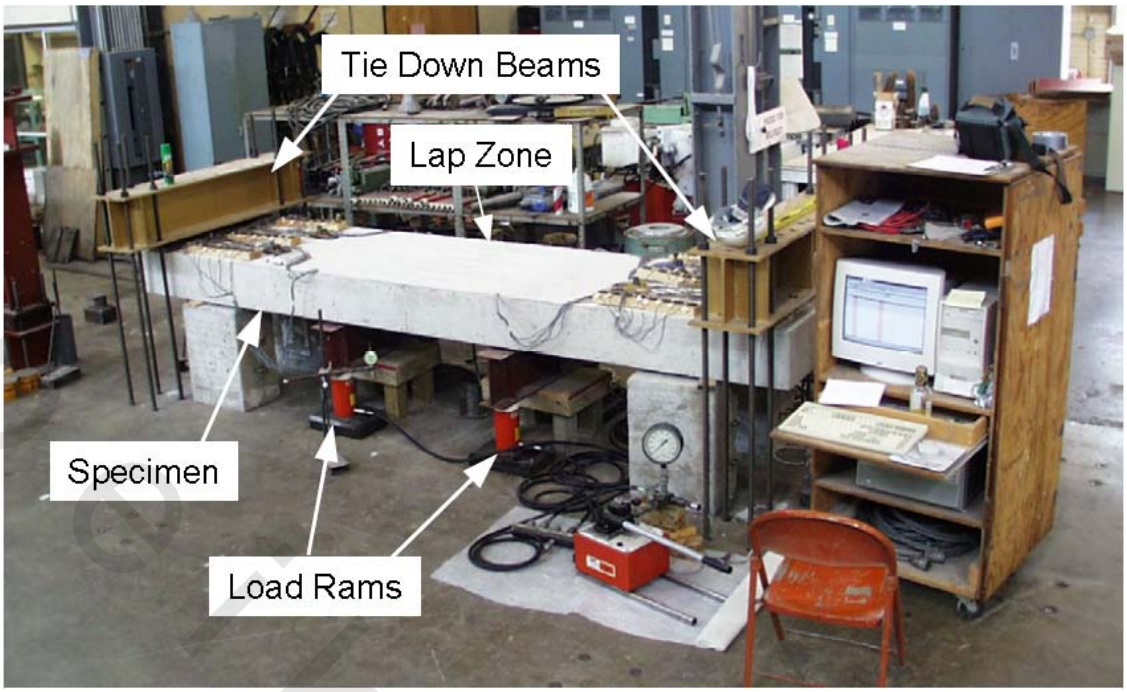

Figure (2-36): A typical lap splice test by Thompson et al (2002) [24]

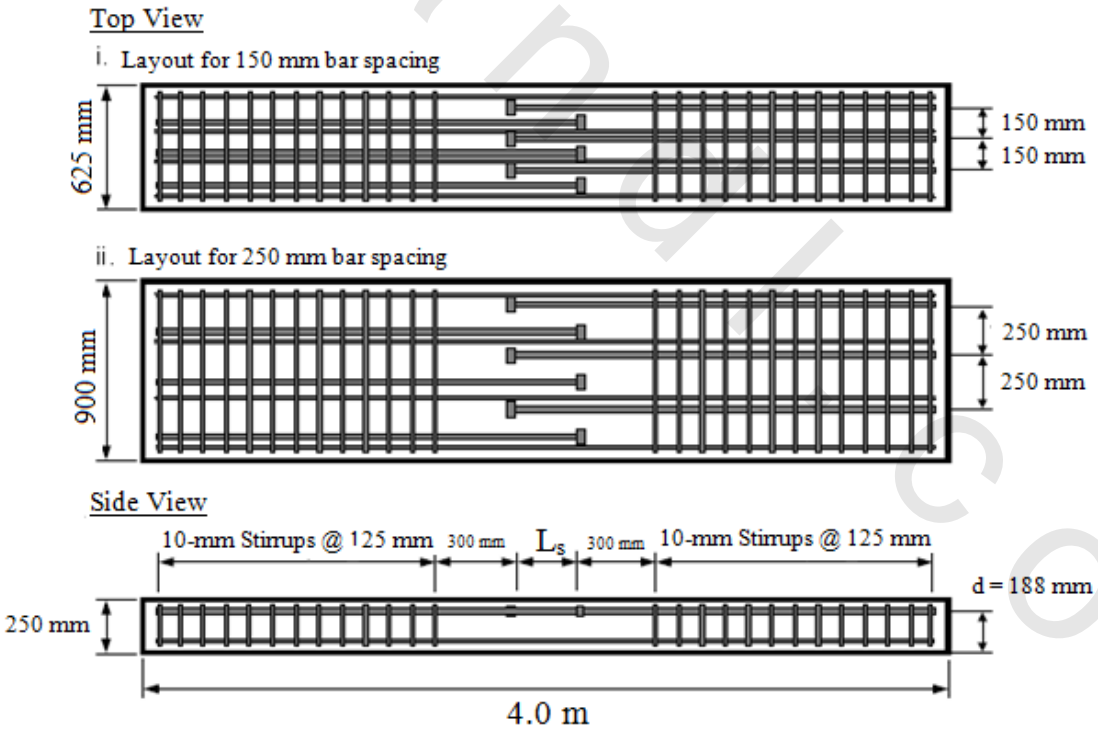

Figure (2-37): Reinforcement details of unconfined lap splice specimens by Thompson et al (2002) [24]

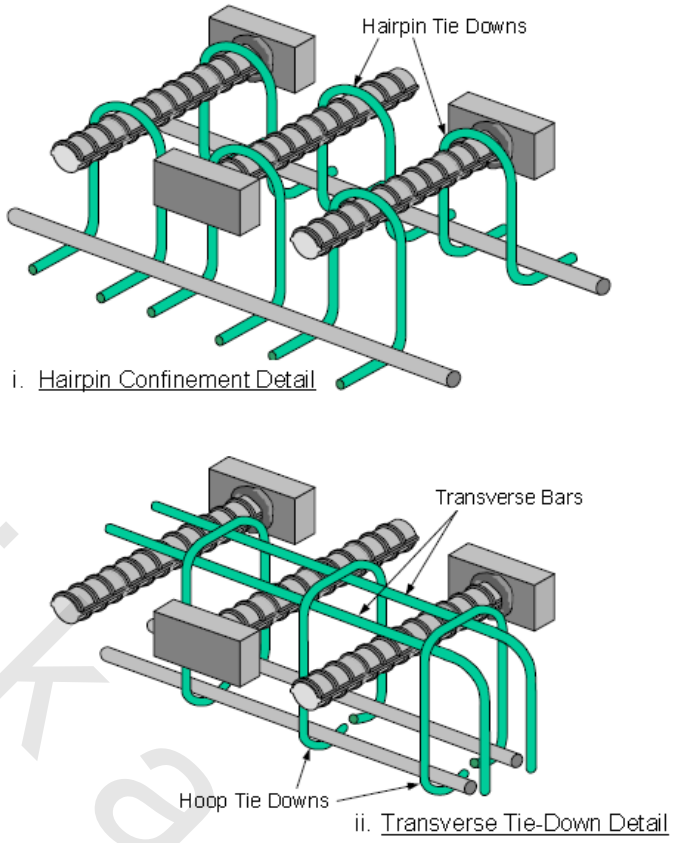

Figure (2-38): The two types of lap splice confinement details tested by Thompson et al (2002) [24]

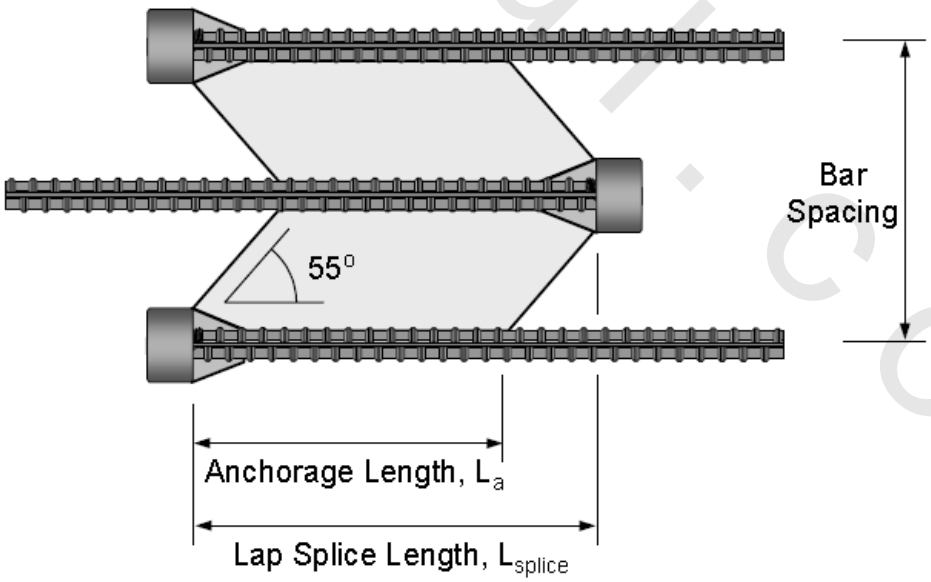

Figure (2-39): Mechanism of stress transfer between lapped bars by Thompson et al (2002) [24]

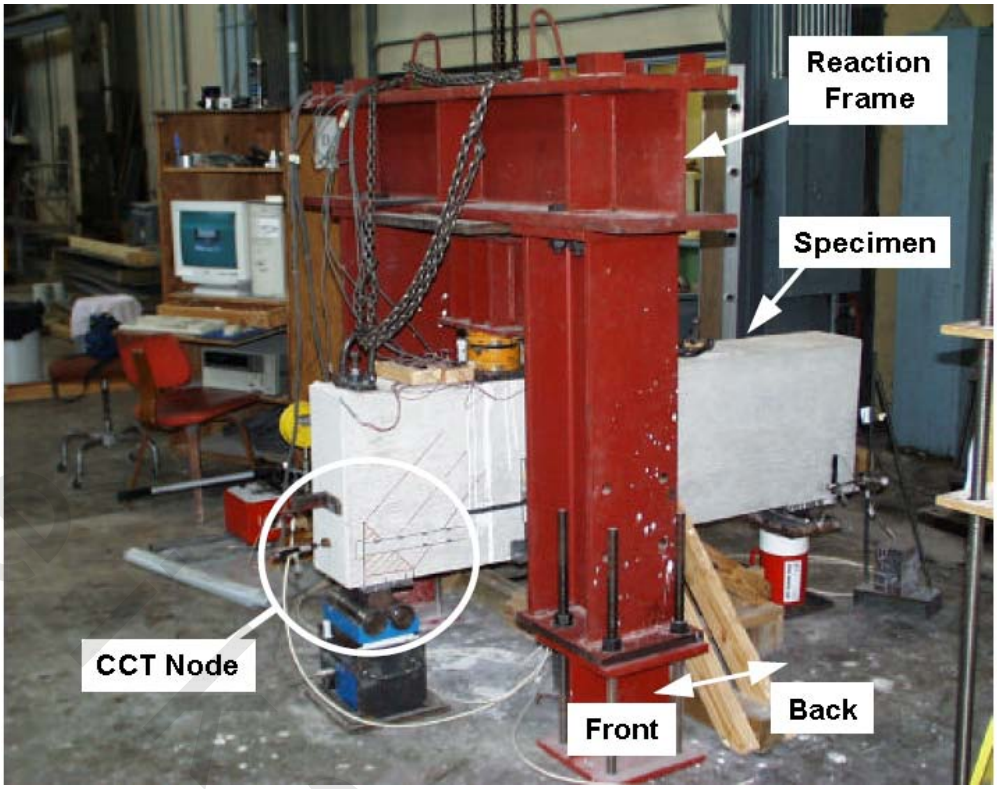

Figure (2-40): A typical CCT node test by Thompson (2002) [22]

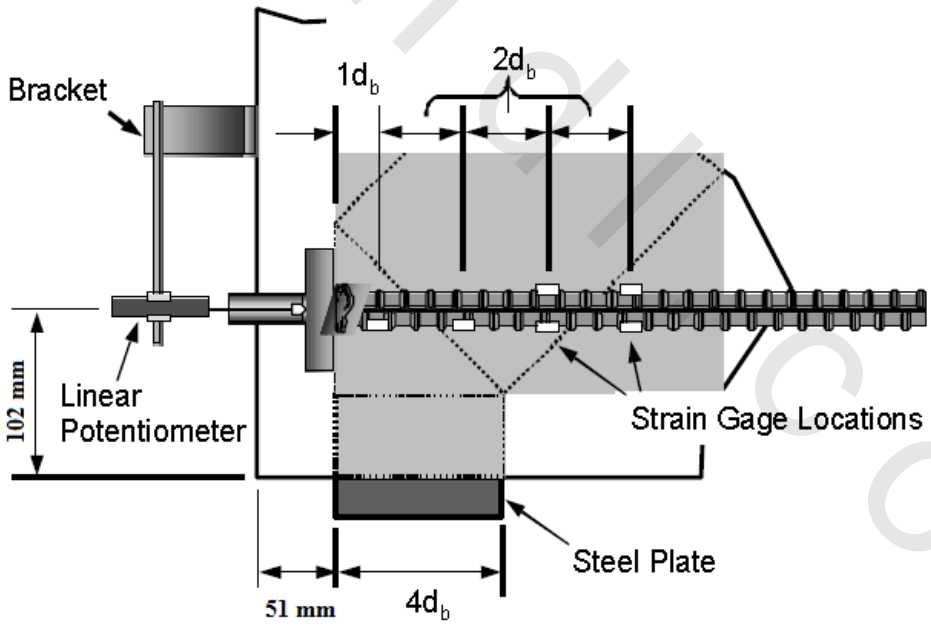

Figure (2-41): Detail of unconfined CCT node by Thompson et al (2002[25], 2005[26], 2006[27])

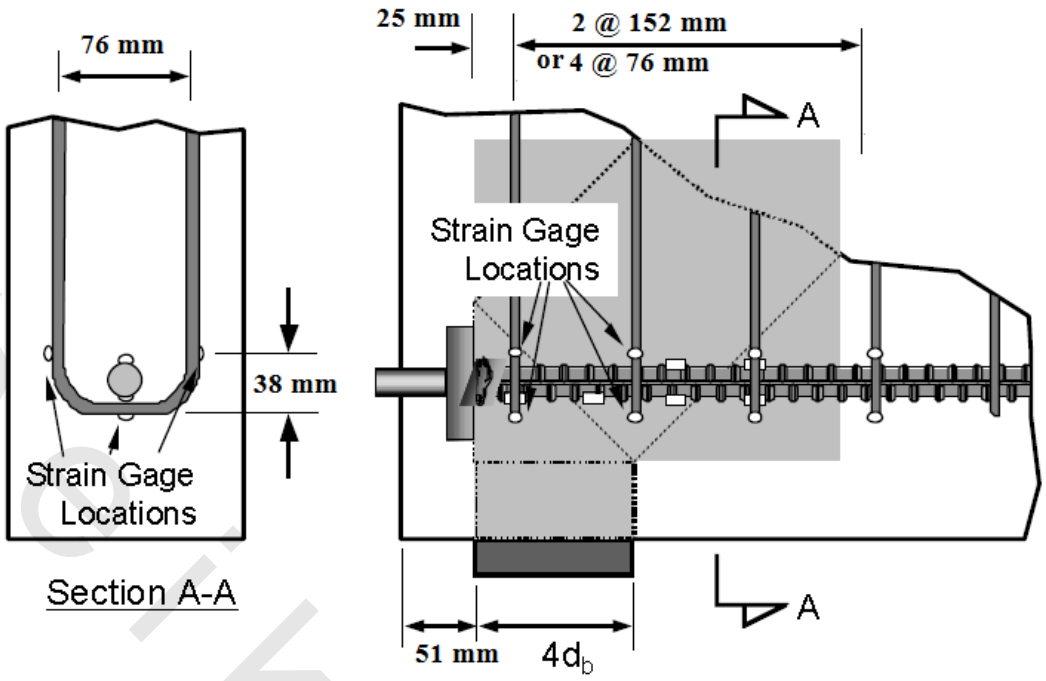

Figure (2-42): Details of confined CCT node specimens by Thompson et al (2002[25], 2005[26], 2006[27])

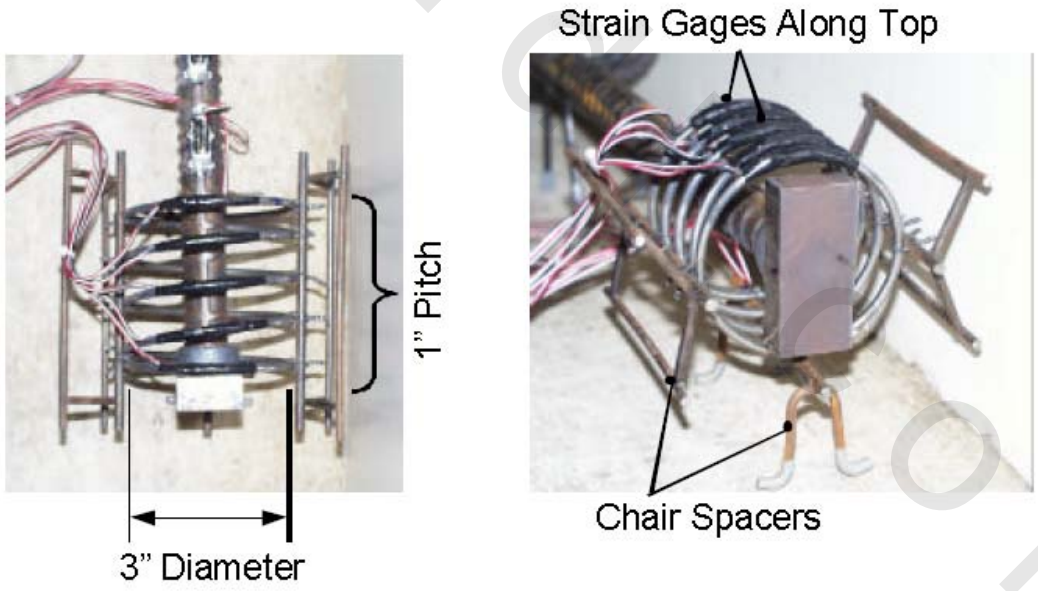

Figure (2-43): Spiral confinement detail in specimen CCT node by Thompson (2002) [22]

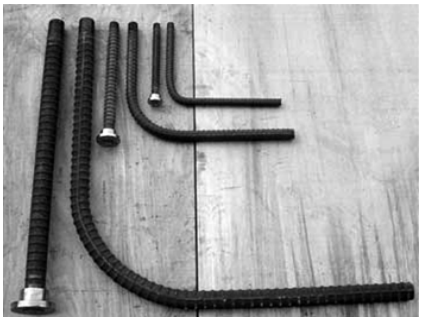

Figure (2-44): Headed bars and hooked bars (No. 8, 11, and No. 18) used by Chun et al (2009) [6]

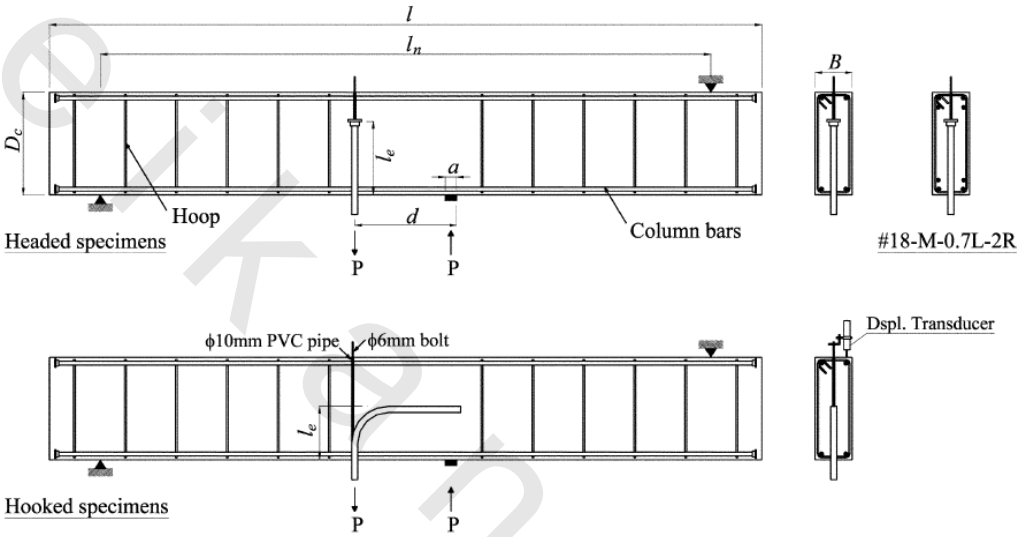

Figure (2-45): Details of specimens tested by Chun et al (2009) [6]

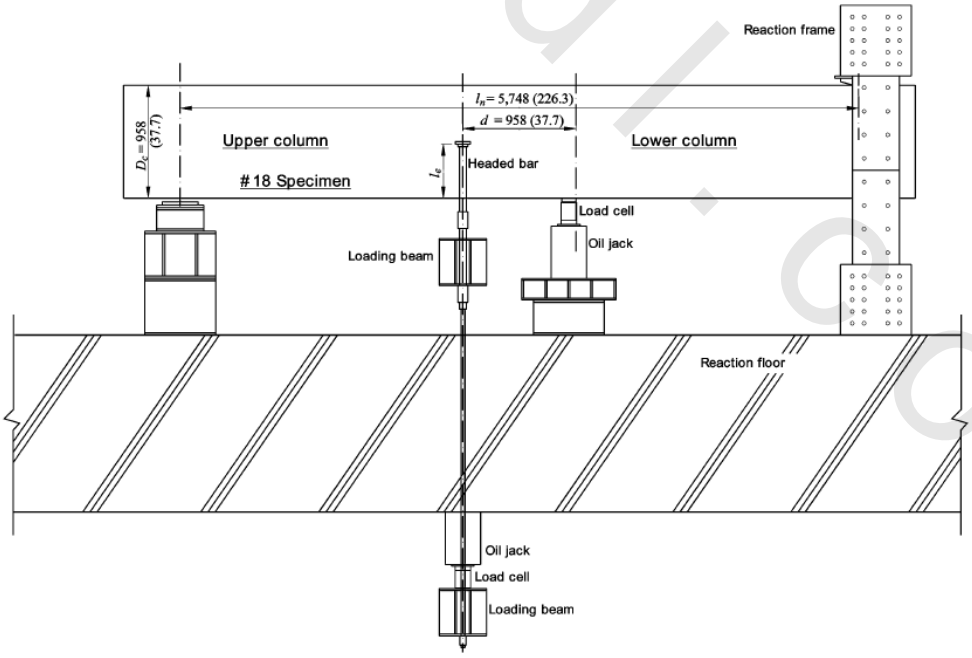

Figure (2-46): Test setup for tests carried out by Chun et al (2009) [6]

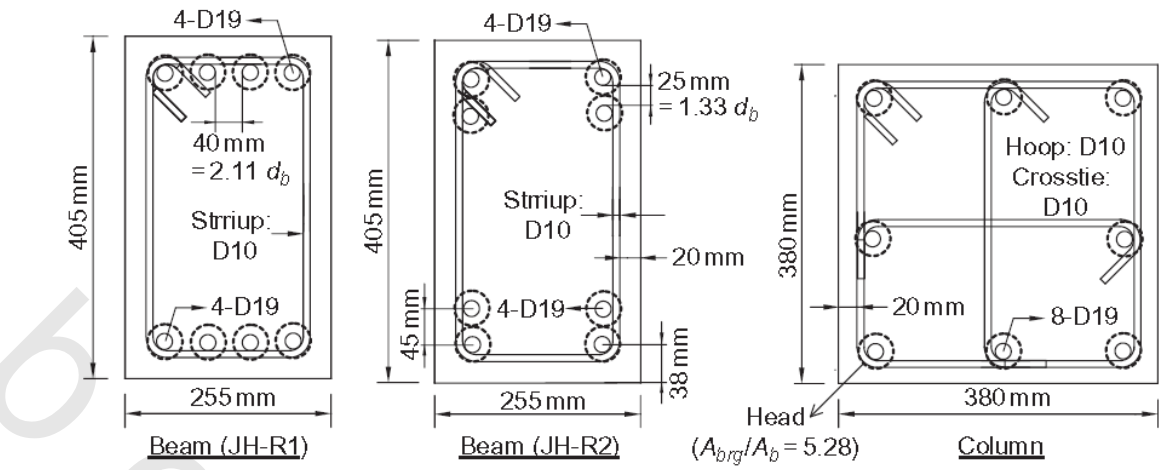

(a) Beam and Column Sections

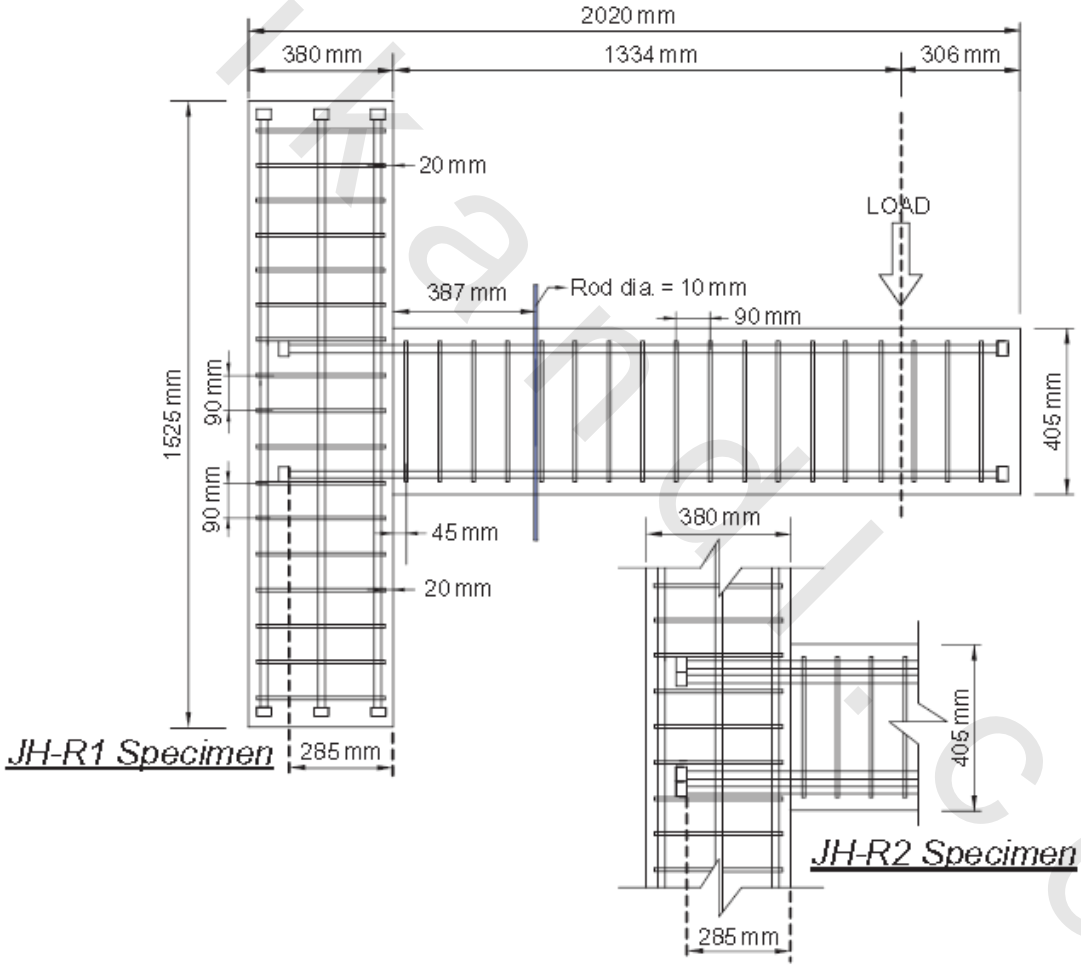

(b) Reinforcement for Joint Subassemblies

Figure (2-47): Dimensions and details for JH-R1 and JH-R2 specimens tested by Kang et al (2012) [16]

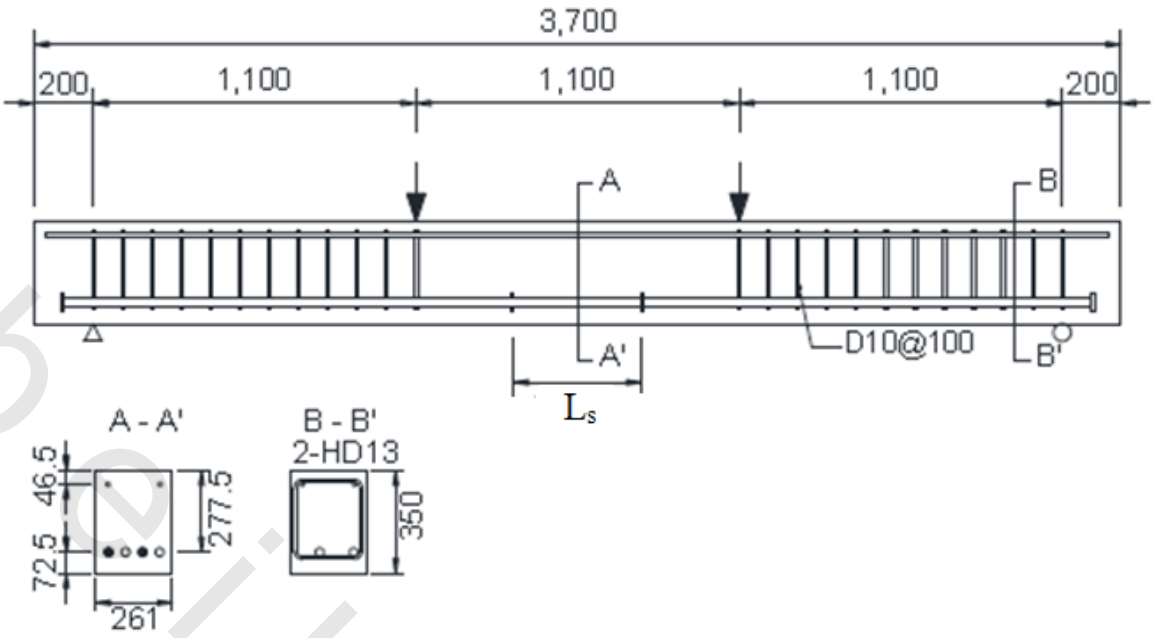

Figure (2-48): Details of lap splice specimen tested by Chun and Lee (2013) [4]

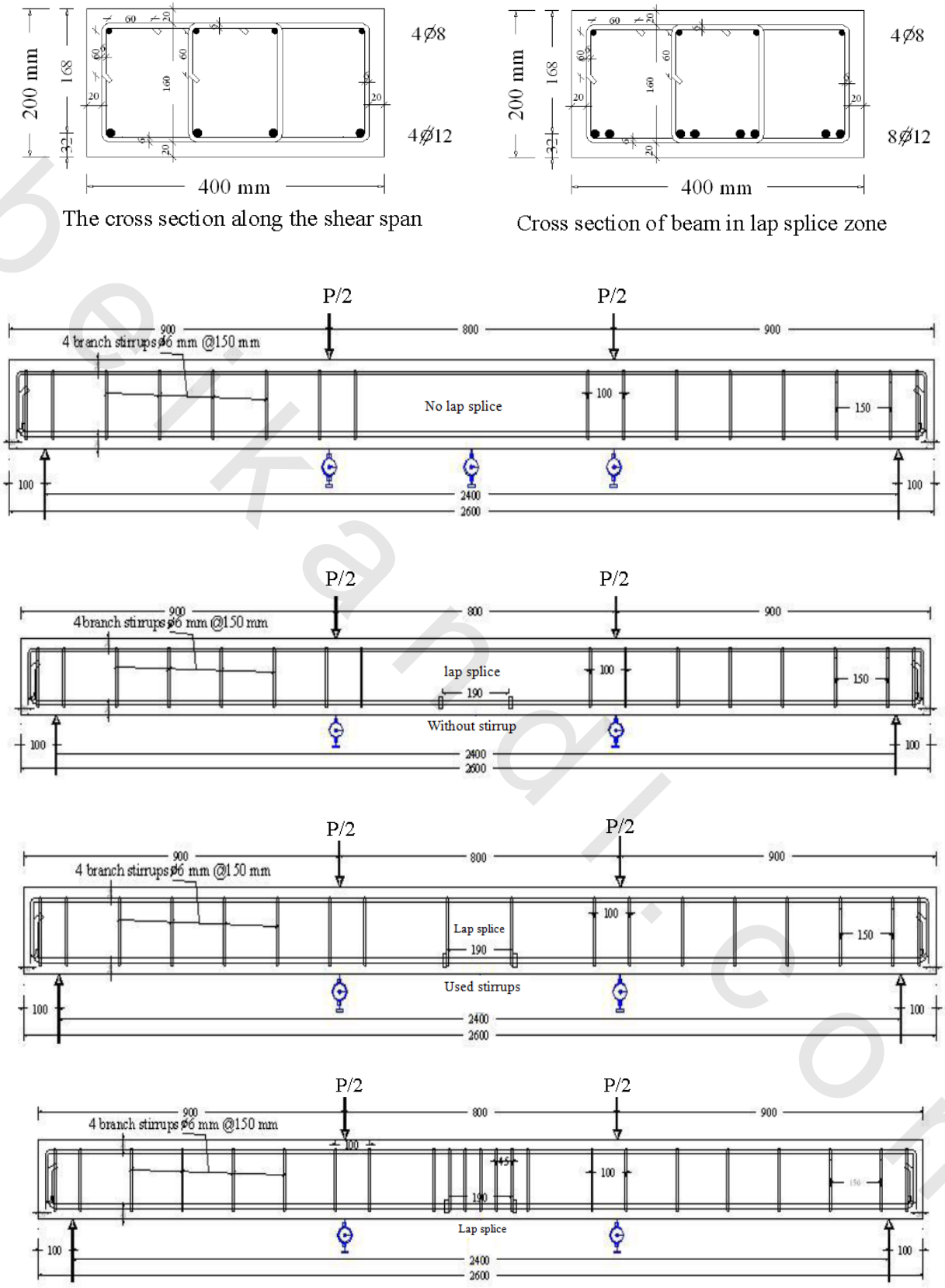

Figure (2-49): Details of some tested specimens by Yassin (2013)[28]

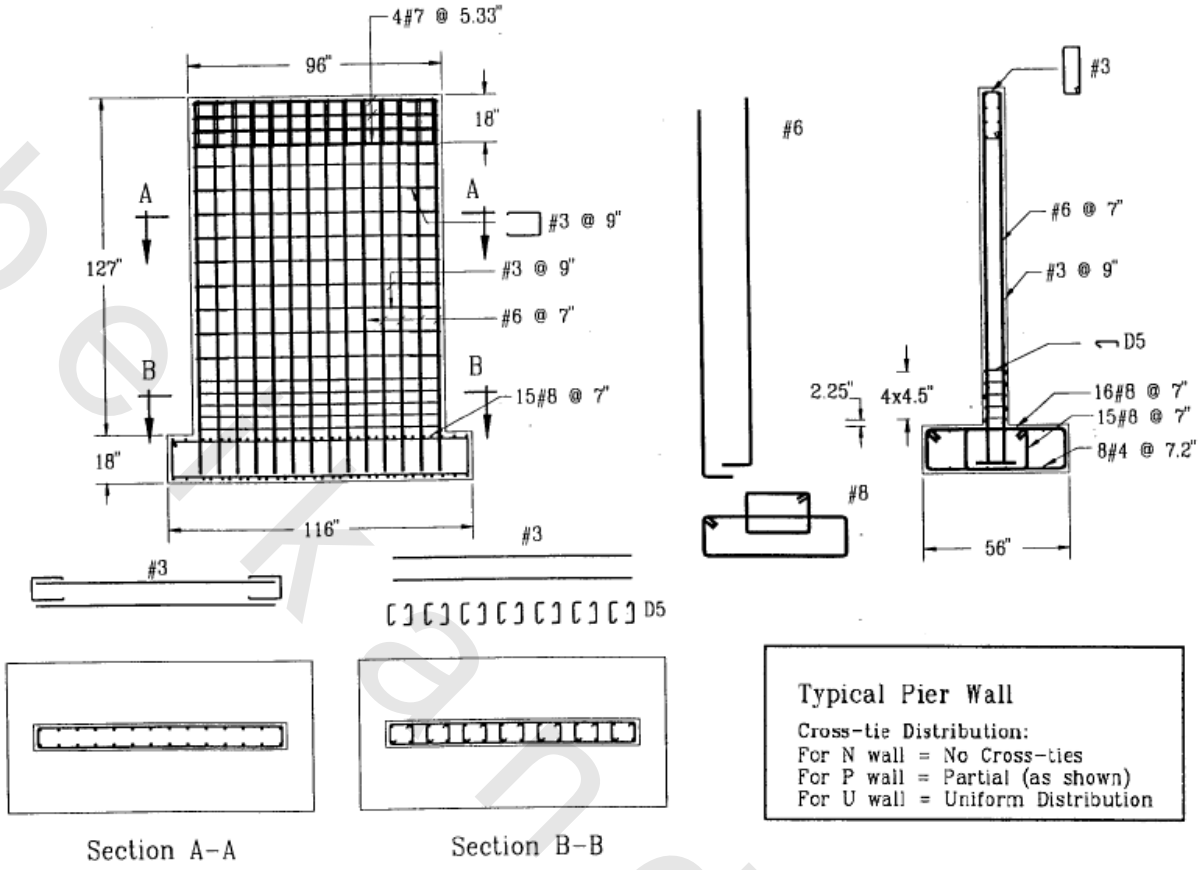

Figure (2-50): Reinforcement details of original pier walls tested by Haroun et al (2000) [15]

Figure (2-51): Repair with alternating crossties by Haroun et al (2000) [15]

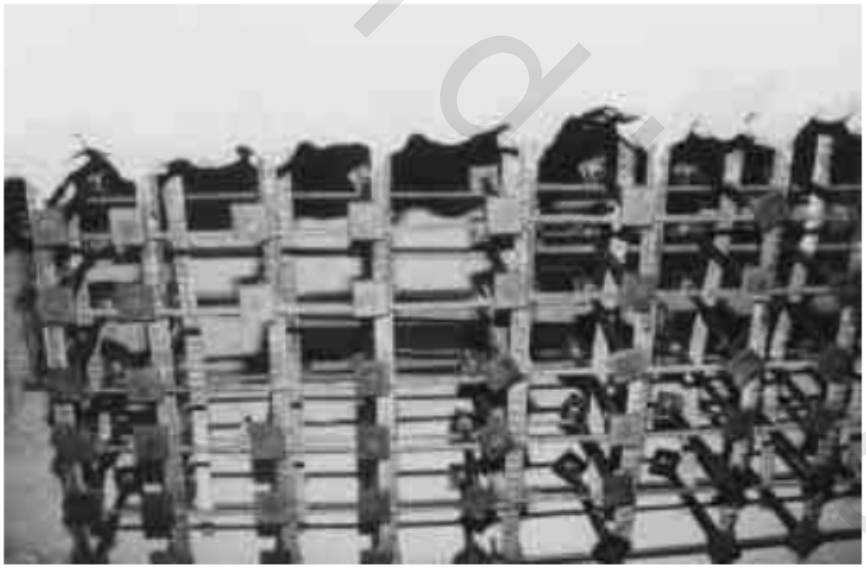

Figure (2-52): Repair with T-headed crossties by Haroun et al (2000) [15]

Figure (2-53): Mechanical Anchor used by Chun and Kim (2004) [5]

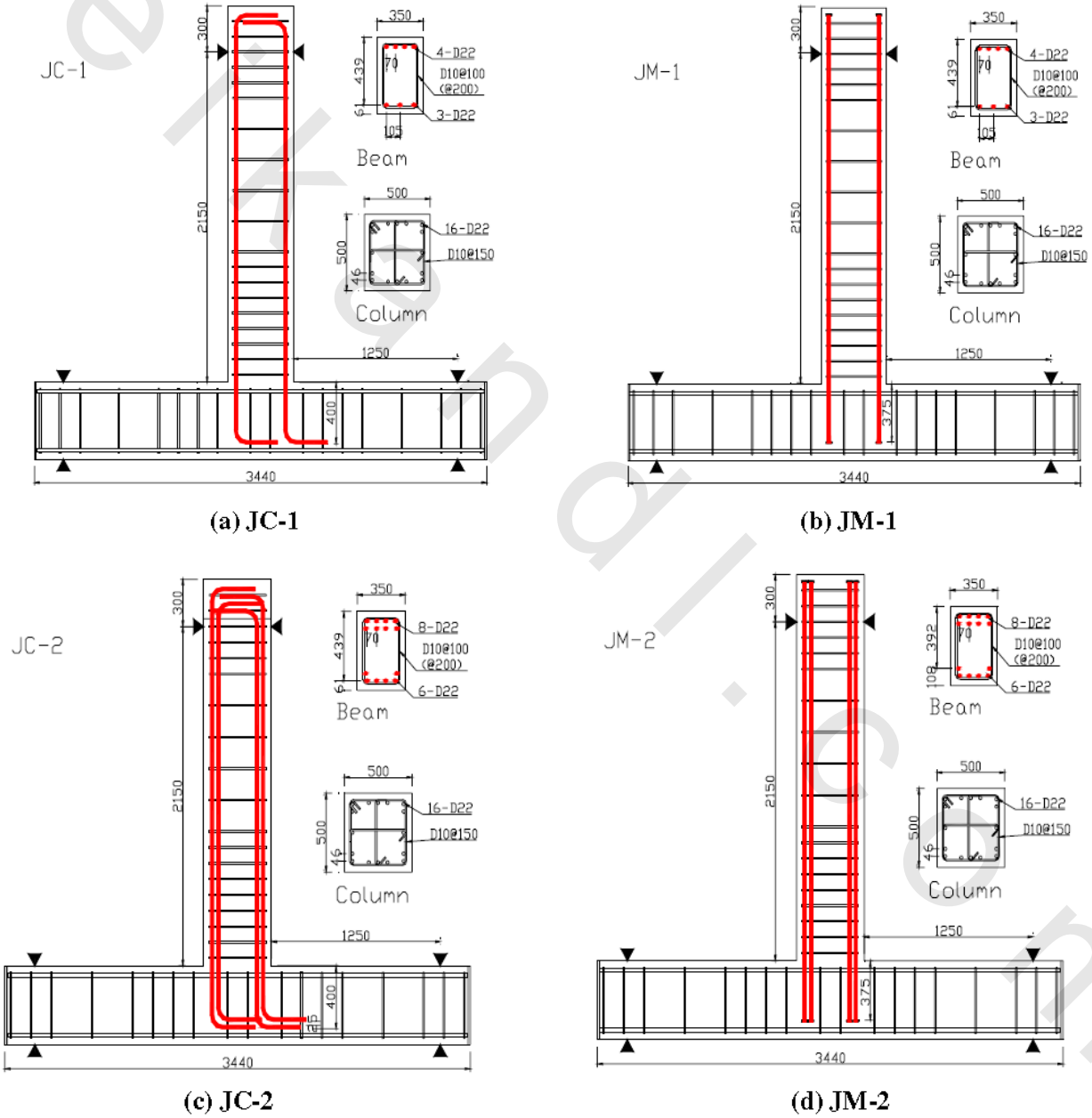

(a) JC-1 (b) JM-1

(c) JC-2 (d) JM-2

Figure (2-54): Details of Specimens tested by Chun and Kim (2004) [5]

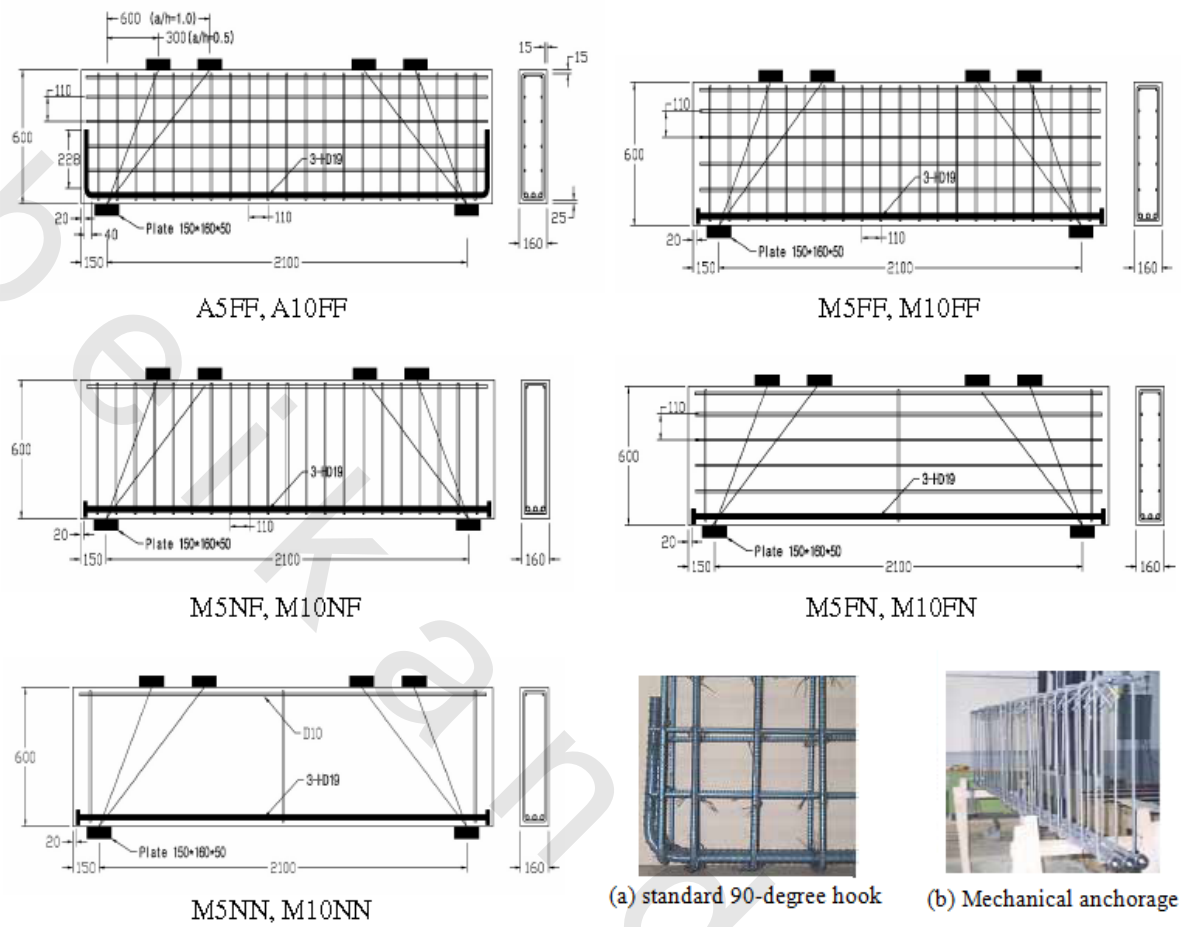

Figure (2-55): Reinforcement details of experimental deep beams by Seo et al (2004) [19]

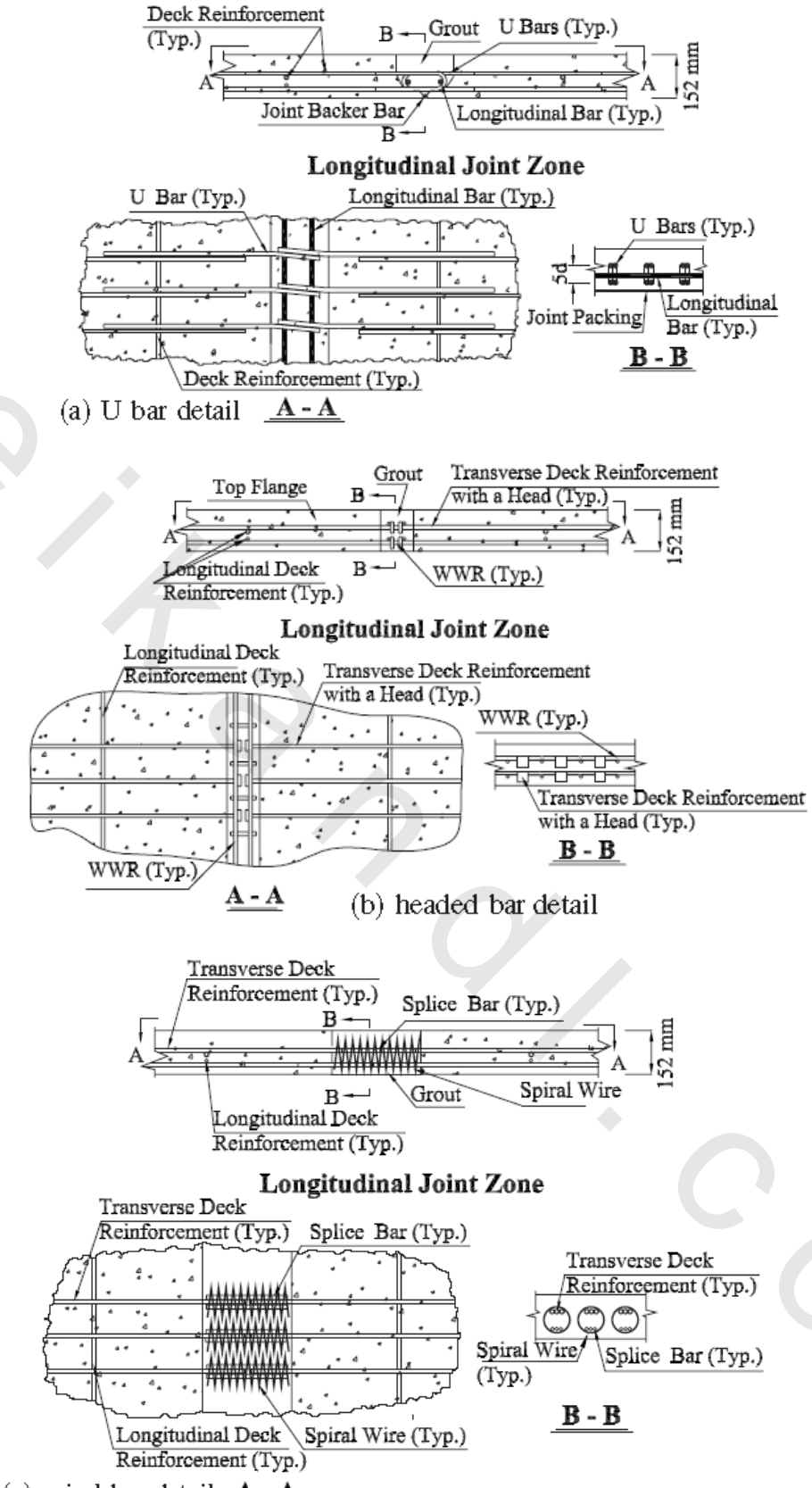

Figure (2-56): Proposed new joint details: (a) U bar detail; (b) headed bar detail; and (c) spiral bar detail by Li et al (2010) [18]

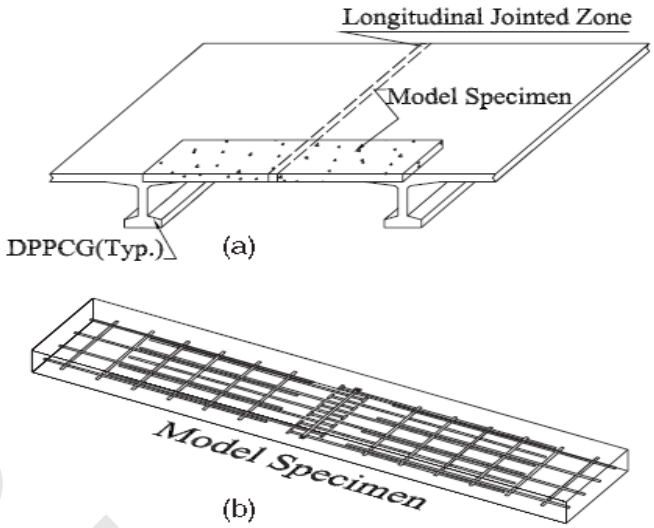

Figure (2-57): Specimen to evaluate joint behavior by Li et al (2010) [18]

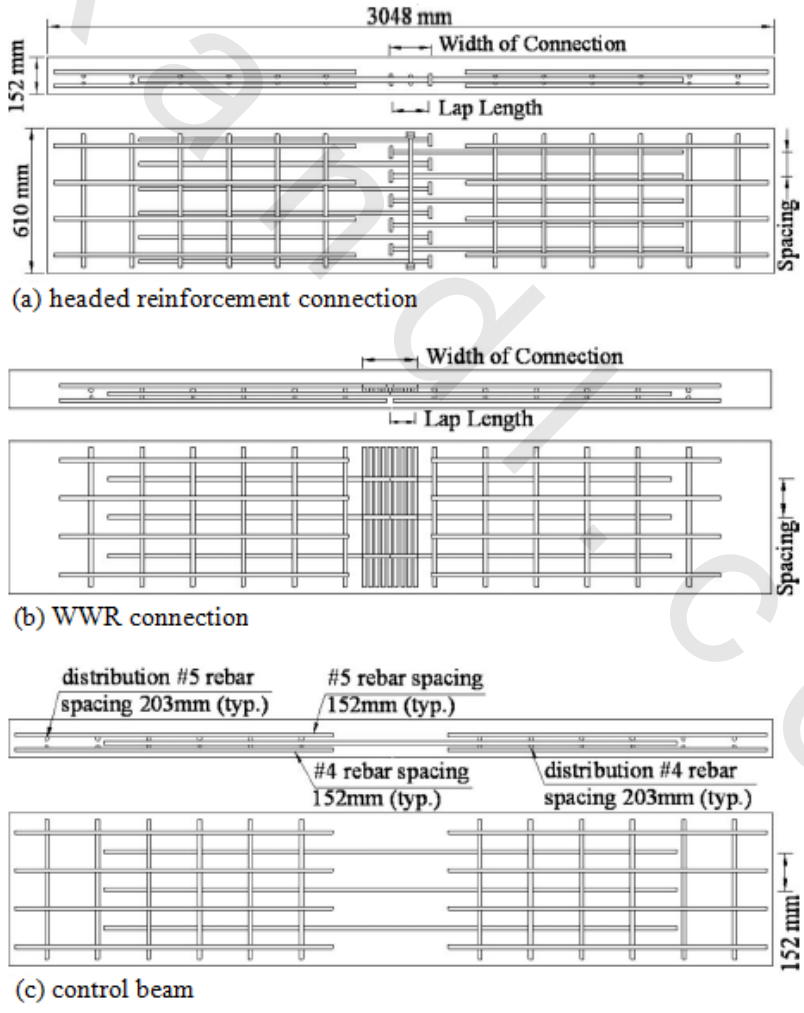

Figure (2-58): Types of specimen tested by Li et al (2010) [18]

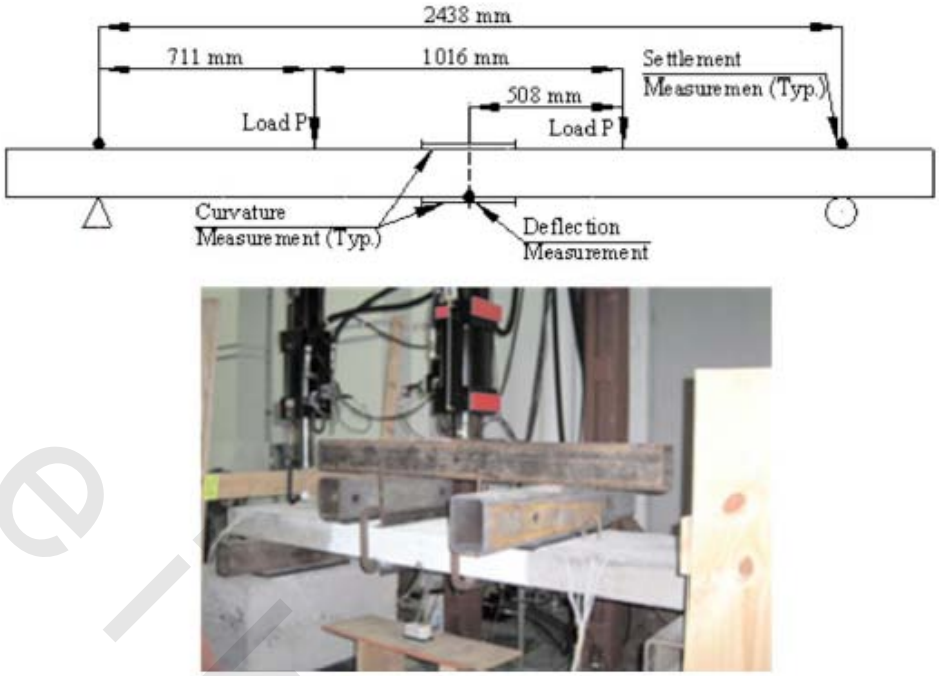

Figure (2-59): Testing setup by Li et al (2010) [18]

(a) ductile failure

(b) brittle failure

Figure (2-60): Failure types within experimental program by Li et al (2010) [18]